The novel role of Kallistatin in linking metabolic syndromes and cognitive memory deterioration by inducing amyloid-β plaques accumulation and tau protein hyperphosphorylation

Weiwei Qi[1,2#], Yanlan Long[3#], Ziming Li[4#], Zhen Zhao[1], Jinhui Shi[1], Wanting Xie[1], Laijian Wang[4], Yandan Tan[1], Ti Zhou[1], Ping Jiang[5*], Bin Jiang[4*], Xia Yang[1,6*], Guoquan Gao[1,7,8,9*]

[1] Department of Biochemistry and molecular biology, Zhongshan School of Medicine, Sun Yat-sen University, Guangzhou, China

[2] Advanced Medical Technology Center, The First Affiliated Hospital, Zhongshan School of Medicine, Sun Yat-sen University

[3] Guangdong Key Laboratory of Nanomedicine, CAS-HK Joint Lab of Biomaterials, Shenzhen Institute of Advanced Technology (SIAT), Chinese Academy of Sciences (CAS), Shenzhen, China

[4] Guangdong Province Key Laboratory of Brain Function and Disease, School of Medicine, Sun Yat-sen University, Shenzhen, China

[5] Department of Clinical Medical Laboratory, Guangzhou First People Hospital, School of Medicine, South China University of Technology, Guangzhou, China

[6] China Key Laboratory of Tropical Disease Control (Sun Yat-sen University), Ministry of Education, Guangzhou, China

[7] Guangdong Engineering & Technology Research Center for Gene Manipulation and Biomacromolecular Products (Sun Yat-sen University), Guangzhou, China

[8] Guangdong Province Key Laboratory of Brain Function and Disease, Zhongshan School of Medicine, Sun Yat-sen University, Guangzhou, China

[9] Guangdong Provincial Key Laboratory of Diabetology& Guangzhou Municipal Key Laboratory of Mechanistic and Translational Obesity Research, Medical Center for Comprehensive Weight Control, The Third Affiliated Hospital of Sun Yat-sen University Guangzhou, Guangdong, China

[#]These authors contributed equally to this study.

*Corresponding author: Gao GQ: gaogq@mail.sysu.edu.cn; Yang X: yangxia@mail.sysu.edu.cn; Jiang B: jiangb3@mail.sysu.edu.cn; Ping J: jiangp45@mail2.sysu.edu.cn

Highlights

- Kallistatin-transgenic(KAL-TG) mice defined its cognitive memory impairment phenotype accompanied by increased Aβ deposition and tau phosphorylation.
- Kallistatin could directly bind to the Notch1 receptor and thereby upregulate BACE1 expression by inhibiting PPARγ signaling.
- Fenofibrate could alleviate cognitive memory impairment and down-regulate the serum Kallistatin level.

Abstract

Accumulation of amyloid β (Aβ) peptides and hyperphosphorylated tau proteins

in the hippocampus triggers cognitive memory decline in Alzheimer's disease (AD). The incidence and mortality of sporadic AD were tightly associated with diabetes and hyperlipidemia, while the exact linked molecular is uncertain. Here, we reported that serum Kallistatin concentrations were meaningfully higher in AD patients, with a higher concentration of fasting blood glucose and triglyceride. In addition, the constructed Kallistatin-transgenic (KAL-TG) mice defined its cognitive memory impairment phenotype and lower LTP in hippocampal CA1 neurons accompanied by increased Aβ deposition and tau phosphorylation. Mechanistically, Kallistatin could directly bind to the Notch1 receptor and thereby upregulate BACE1 expression by inhibiting PPARγ signaling, resulting in Aβ cleavage and production. Besides, Kallistatin could promote the phosphorylation of tau by activating GSK-3β. Fenofibrate, a hypolipidemic drug, could alleviate cognitive memory impairment by down-regulating Aβ and tau phosphorylation of KAL-TG mice. Collectively, our data clarified a novel mechanism for Aβ accumulation and tau protein hyperphosphorylation regulation by Kallistatin, which might play a crucial role in linking metabolic syndromes and cognitive memory deterioration, and suggested that fenofibrate might have the potential for treating metabolism-related AD.

Key words: Alzheimer's disease, Kallistatin, Aβ42, BACE1, Diabetes

62 **Introduction**

63 Alzheimer's disease (AD), the most common irreversible neurodegenerative
64 disease involving dementia in the elderly, is characterized by progressive deterioration
65 of cognitive memory. Pathologically, the characteristic hallmarks of AD are
66 extracellular amyloid-β (Aβ) plaques and intracellular neurofibrillary tangles (NFTs)
67 [1, 2, 3]. Aβ cascade and the hyperphosphorylation of tau protein are two main
68 hypotheses related to AD. The Aβ cascade hypothesis dominates that overproduction
69 of Aβ changes the normal cellular state, resulting in synaptic dysfunction,
70 neurodegeneration, tau hyperphosphorylation, and neuroinflammation, eventually
71 causing memory loss in AD and dementia patients [4, 5]. Aβ peptides are produced from
72 the sequential cleavage of amyloid precursor protein (APP) by β-secretase (β-site APP
73 cleaving enzyme 1, BACE1) and γ-secretase, therefore this cleavage step contributes
74 heavily to AD pathology [6, 7]. BACE1 is one of the most potential therapeutic targets.
75 Some potent BACE1 inhibitors have advanced to late stages in clinical trials,
76 highlighting the significance of BACE1 in the Aβ generation [8, 9, 10]. Tau is a protein
77 found in microtubules. It exists physiologically in axons and regulates microtubule
78 dynamics and axonal transport [11]. Tau goes through a multi-step process in AD,
79 transitioning from a natively unfolded monomer to massive aggregated aggregates
80 like NFTs, another hallmark of AD [12, 13]. One of the central kinases responsible for
81 initiating tau phosphorylation is glycogen synthase kinase-3 (GSK3) and Wnt
82 signaling play a vital role in activating GSK-3β and GSK-3β-mediated tau

83 phosphorylation [14]. The physiological mechanisms governing their relationship are
84 still poorly understood.

85 There has been a close relationship between metabolic disorders and cognitive
86 impairment across the AD spectrum [15, 16]. Accounting for nearly 95% of AD patients
87 were categorized as sporadic ones, whose increasing incidence and mortality were
88 tightly associated with type 2 diabetes mellitus (T2DM), obesity, and hyperlipidemia
89 [17, 18, 19]. There was about 37 percent comorbidity between AD and diabetes reported
90 by the Alzheimer's Association Report [20, 21]. As a result of the strong association and
91 share mechanism between AD and T2DM, AD was termed "Type 3 Diabetes" by
92 some researchers [22, 23, 24, 25]. Several studies demonstrate that diabetes confers a 1.6-
93 fold increased risk of developing dementia [26, 27]. Similarly, central obesity and high
94 body mass index (BMI) during middle age have about 3.5 times increased risk of
95 dementia later in life [28]. Therefore, control of blood glucose and lipids is expected to
96 be a strategy for preventing or moderating cognitive decline in aging. Nevertheless,
97 the exact link and key associated regulator between metabolic abnormalities and AD
98 is still unclear.

99 Kallistatin was a serine proteinase inhibitor, previously identified as a tissue
100 kallikrein-binding protein [29]. It was predominantly produced in the liver and widely
101 expressed in the body tissues and conferred anti-angiogenesis, anti-fibrosis, anti-
102 oxidative stress, and anti-tumor growth [30, 31]. Furthermore, Kallistatin was found
103 increased in patients with obesity, prediabetes, and diabetes [32, 33, 34]. The concentration

104 of Kallistatin was positively correlated with the triglyceride glucose index [35], which
105 was proven to be an independent risk factor for dementia [36]. In addition, our previous
106 study revealed that the concentration of serum Kallistatin in T2DM patients was
107 significantly increased and further clarified that Kallistatin suspended wound healing
108 in T2DM patients by promoting local inflammation, which suggested that Kallistatin
109 played a critical role in the progression of T2DM [37]. Furthermore, our recent research
110 has found that kallistatin can cause memory and cognitive dysfunction by disrupting
111 the glutamate-glutamine cycle[38].

112 According to the relationship between T2DM, AD and Kallistatin, we
113 constructed Kallistatin transgenic (KAL-TG) mice to explore whether it could cause
114 cognitive impairment through up-regulation of Aβ production. Taken together, our
115 results suggest that a novel regulatory mechanism of Aβ production and tau protein
116 hyperphosphorylation by Kallistatin is involved in the progression of metabolic
117 abnormalities-related AD.

118

119 **Results**

120 **Kallistatin was increased in AD patients and AD model mice.**

121 To explore the relevance of AD in T2DM (Fig.S1A), we first performed a GAD
122 disease enrichment analysis of differentially expressed genes in neurons of T2DM and
123 normal controls, and found AD was closely related to T2DM (GSE161355). We
124 further identified enrichment of the Serpin family protein domain using PFAM

125 analysis on the David database (Fig.S1B) (https://david.ncifcrf.gov/). Our previous
126 studies found that Kallistatin (serpin family a member 4) was elevated in the serum of
127 T2DM patients and caused an adverse prognosis of diabetes complications [44]. We
128 have collected 11 serum samples of dementia patients from Sun Yat-sen Memorial
129 Hospital and found that the concentration of Kallistatin was higher compared to the
130 normal control[38]. Here, we enrolled 56 AD patients and 61 healthy controls from four
131 hospitals in Guangdong province to further explore the potential relevance of
132 Kallistatin and AD. The Clinical and biochemical characteristics are presented in
133 Table S1, S2. In addition, we measured the serum Kallistatin (12.78±2.80 μg/ml)
134 content in patients with AD was higher than in normal controls (9.78±1.93 μg/ml)
135 (Fig.1A). Likewise, the fasting blood glucose (FBG) and triglyceride (TG) were more
136 elevated in AD patients than in healthy human (Fig. 1B). We further grouped all the
137 AD patients according to whether they had diabetes, then found Kallistatin
138 (13.79±3.05 μg/ml) and TG content were further elevated in AD patients with
139 diabetes (Fig.1C-D). Similarly, Kallistatin expression was increased in AD model
140 mouse SAMP8 compared with its control mouse SAMR1 in hippocampus tissue
141 (Fig.S1C-D). Taken together, these results indicated that Kallistatin concentration was
142 increased in metabolic abnormalities-related AD patients.

143 **Kallistatin could impair cognitive memory in mice.**

144 The above experiments proved that Kallistatin increased in AD patients and AD
145 model mice. Then, we constructed KAL-TG mice and assessed their behavioral

146 performance through the Morris water maze (MWM) and Y-maze tests. Notably, the
147 latency to escape platform was increased, and crossing platform times, time in
148 percent, and spontaneous alternation were significantly decreased in KAL-TG mice
149 compared with age-matched WT mice (Fig.1E-I). Furthermore, long-term potentiation
150 (LTP) was measured by whole-cell voltage-clamp recordings of CA1 neurons in acute
151 hippocampal slices of KAL-TG and WT mice to determine the changes in
152 hippocampal synapses. LTP of KAL-TG mice was significantly lower than WT mice
153 (Fig.1J). These results showed Kallistatin could impair cognitive memory in mice.

154 **Kallistatin promoted Aβ deposition and tau phosphorylation.**

155 We evaluated Aβ deposition and tau phosphorylation in these experimental mice
156 hippocampus tissues by immunohistochemistry staining and western blot. Predictably,
157 the plaque density and tau phosphorylation of KAL-TG mice were much higher than
158 age-matched WT mice (Fig.2A-C, 3A-D). Consistent with this result, ELISA
159 detection of Aβ42 contents in hippocampus tissue showed that Aβ production was
160 extraordinarily increased in KAL-TG mice compared to WT mice (Fig.2D). These
161 results suggested that Kallistatin promoted Aβ deposition and tau phosphorylation.

162 **Kallistatin positively regulated Aβ generation by promoting β-secretase rather**
163 **than γ-secretase.**

164 Western blot and ELISA analysis of Aβ levels in primary hippocampal neurons
165 (immunofluorescence identified with neural marker MAP2, Fig.S2G) infected with
166 overexpressing Kallistatin adenovirus were higher than in control groups (Fig.2E-G),

167 as well as HT22 cells (Fig.S2A-C). Amyloid-beta precursor protein (APP) undergoes
168 proteolytic processing to generate peptide fragments [45]. β-secretase (BACE1) and γ-
169 secretase, composed of presenilin 1 (PS1), nicastrin, and Pen-2, were crucial enzymes
170 for Aβ generation [46, 47]. We determined the levels of APP, BACE1, and PS1 in
171 hippocampus tissue. BACE1 protein and mRNA accumulate to higher levels in KAL-
172 TG mice compared with WT mice (Fig.4A-C, S2D, whereas no significant difference
173 appeared in APP, PS1, and α-secretases (ADAM9, ADAM10, and ADAM17)
174 expression (Fig.4A, S2E). Consistent with the above results, the activity of BACE1
175 was increased (Fig.4D), while PS1 activity was not changed (Fig.S2F). Similarly, the
176 expression and activity of BACE1 were further determined to increase in primary
177 mouse neurons, and HT22 cells transfected with Kallistatin adenovirus (Fig.5A-C,
178 S3A-C), and PS1 expression and activity were still not changed (Fig.5A, 5D, S3A).
179 Furthermore, the effect of Kallistatin was attenuated by the BACE1 inhibitor
180 (verubecestat) or siBACE1 03, the most effective one (Fig.5E-F, S3D). Therefore,
181 these results indicated that Kallistatin could promote Aβ generation through
182 upregulating BACE1 expression.

183 **Kallistatin suppressed PPARγ activation to promote BACE1 expression.**

184 Transcription factors SP1, YY1, and PPAR were reported to regulate BACE1
185 expression at the transcription level. Among them, PPARγ could down-regulated
186 BACE1 expression [48, 49, 50]. As elaborated, PPARγ decreased in the hippocampal tissue
187 of KAL-TG mice detected by western blot and immunohistochemical analysis

188 (Fig.5G-J). However, no statistical differences appeared in the YY1 and SP1
189 expressions (Fig.5G). In addition, Kallistatin downregulated the expression of PPARγ
190 on primary hippocampal neurons and HT22 cells, thus increasing BACE1 and Aβ
191 expression (Fig.5K, S3E). Treatment with rosiglitazone, the PPARγ agonist, could
192 reverse the decrease of PPARγ caused by Kallistatin (Fig.5K-L). Predictably,
193 rosiglitazone could inhibit the promoting effect of Kallistatin on BACE1 and Aβ
194 (Fig.5K and Fig.S3E).

195 **Kallistatin promoted Aβ production *via* directly binding to the Notch1 receptor**
196 **and activating the Notch1 pathway.**

197 Our results indicated that Notch1 was highly expressed in the hippocampal
198 tissues of KAL-TG mice (Fig.6A-D). Moreover, primary hippocampal neurons and
199 HT22 cells infected with overexpressing Kallistatin adenovirus had upregulated
200 Notch1 expression *in vitro* (Fig.S4A-B). In addition, Kallistatin could directly bind to
201 the Notch1 receptor and activate the Notch1 pathway (Fig.6E-F and Fig.S4C-D).
202 Treatment with the siNotch1 03, which was the most effective (Fig.S4E), to knock
203 down Notch1 inhibited the effect of Kallistatin on the activation of the Notch1
204 signaling pathway, resulting in the downregulation of HES1, upregulation of PPARγ,
205 and downregulation of BACE1 and Aβ (Fig.6G). HES1, an essential downstream
206 effector of Notch1 signaling pathway, was reported to suppress the expression
207 of *PPARG* (gene name of PPARγ) in neuron cells [51, 52]. Similarly, the HES1 shRNA
208 01, the most effective (Fig.S4F), could upregulate PPARγ and decrease the production

209 of BACE1 and Aβ when the neuron cells are infected with adenovirus to overexpress
210 Kallistatin (Fig.6H). The above results suggested that Kallistatin promotes Aβ
211 production *via* directly binding to the Notch1 receptor and activating the Notch1
212 pathway.

213 **Kallistatin promoted the phosphorylation of tau by activating the Wnt signaling**
214 **pathway.**

215 Glycogen synthase kinase 3-β (GSK-3β) is a crucial element in the
216 phosphorylation of tau [53]. When the Wnt signaling was activated, LRP6 PPPSPxS
217 motif could directly interact with GSK3-3β and phosphorylate it [54]. So when the Wnt
218 signaling was inhibited, GSK3β was activated and dephosphorylated, and non-
219 phosphorylated GSK3β was able to add phosphate groups to serine/threonine residues
220 of tau [14]. Kallistatin has already been reported as a competitive inhibitor of the
221 canonical Wnt signaling pathway [55]. Consistent with previous reports, our results
222 showed that GSK-3β was activated in the hippocampus of KAL-TG mice (Fig.7A-B).
223 Furthermore, visible increase in tau phosphorylation with the activation of GSK-3β
224 stimulated by Kallistatin overexpression (Fig.7C-D), which could be reversed by
225 LiCl, the inhibitor of GSK-3β (Fig. 7E-F). These results proved that Kallistatin could
226 promote the phosphorylation of tau by activating the Wnt signaling pathway.

227 **Fenofibrate could alleviate memory and cognitive impairment of KAL-TG mice.**

228 Hyperlipidemia and hyperlipidemia were account for the development of AD [56,
229 57]. Here, a hypolipidemic drug (fenofibrate) and a hypoglycemic drug (rosiglitazone)

230 were used to treat the KAL-TG mice (Fig.8A). After a-month treatment with
231 fenofibrate, the behavioral performance measured by MWM and Y-maze test of
232 treated group was improved compared to KAL-TG group. The latency to the escape
233 platform on the fifth training day was significantly decreased (Fig.8B), and crossing
234 platform times (Fig.8C), time in percent (Fig.8D), and spontaneous alternation
235 (Fig.8F) were significantly increased in the fenofibrate-treated group, which
236 performed better than rosiglitazone-treated group. Similarly, the path traces heatmap
237 indicated mice stayed in the target quadrant longer in the fenofibrate-treated group
238 (Fiure.8E). Besides, the decreased serum Kallistatin level, Aβ, BACE1,
239 phosphorylation of tau, and the activation of GSK3β was detected in the fenofibrate-
240 treated KAL-TG group (Fig.8G-I). However, no significant difference showed in the
241 rosiglitazone-treated group compared with the KAL-TG mice (Fig.8G-I).

242 **Mechanism summary**

243 In metabolic abnormalities-related AD patients, the concentration of Kallistatin is
244 elevated, which could increase Aβ deposition through Notch1/HES1/PPARγ/BACE1
245 pathway, and induce tau hyperphosphorylation by activating GSK-3β. Finally,
246 elevated Kallistatin caused impaired cognitive memory via inducing Aβ deposition
247 and tau hyperphosphorylation (Fig.8J).

248

249 **Discussion**

250 This study demonstrated that Kallistatin is a novel regulator of amyloid-β plaque
251 accumulation, tau protein hyperphosphorylation, and metabolic abnormalities-related
252 cognitive memory impairment. We proved that Kallistatin was increased in the serum
253 of AD and diabetes-related AD patients and the hippocampus of AD model mice. In
254 addition, the constructed KAL-TG mice defined its cognitive memory impairment
255 phenotype and lower LTP in hippocampal CA1 neurons accompanied by increased Aβ
256 deposition and tau phosphorylation. Mechanistically, Kallistatin transcriptionally
257 upregulates BACE1 expression by suppressing the transcriptional repressor PPARγ,
258 resulting in Aβ cleavage and production. Most importantly, our studies proved
259 Kallistatin could bind to the Notch1 receptor directly and activate the Notch1/HES1
260 pathway, causing the decrease of PPARγ, overproduction of BACE1, and elevated
261 Aβ42 generation. Moreover, Kallistatin could induce tau phosphorylation by
262 activating GSK-3β, which result from the inhibition of LRP6. Finally, prolonged
263 stimulation with high concentrations of Kallistatin could impair cognitive memory in
264 mice. Lastly, the hypolipidemic drug-fenofibrate decreasing of Aβ expression,
265 phosphorylation of tau, and the serum Kallistatin level of KAL-TG mice, causing
266 alleviating memory and cognitive impairment. For the first time, these observations
267 established an association between high Kallistatin levels and metabolic
268 abnormalities-related AD, and provided a new drug candidate (fenofibrate) for AD
269 patients with metabolic syndromes.

270 Growing shreds of evidence suggest that Diabetes mellitus and AD are closely

271 linked. Approximately 80% of AD subjects are insulin resistant or T2DM [58];
272 additionally, the T2DM patients had a higher risk of up to 73% of dementia than the
273 healthy control population [26]. In line with these observations, the process of cognitive
274 decline in T2DM patients appears to begin in the prediabetic phase of insulin
275 resistance [59, 60]. We performed a GAD disease enrichment analysis of differentially
276 expressed genes in neurons of T2DM and normal controls, which showed AD is
277 closely related to T2DM, besides identified enrichment of the Serpin family protein
278 domain using PFAM analysis (Fig.S1A, B). We and other researchers found that
279 Kallistatin (which belongs to the Serpin family) was increased in T2DM [32, 37].
280 Although the interrelationship between Kallistatin and AD has not been reported to
281 date, we have enough reason to speculate Kallistatin might be one of the critical
282 molecules which could establish the relationship between Alzheimer's disease and
283 Diabetes. Our data suggested that AD patients indeed have metabolic disorders and
284 elevated Kalllistatin (Fig.1A-D, S1C-D). In addition, memory cognitive function and
285 synaptic plasticity of KAL-TG mice were impaired (Fig.1E-J). These results
286 suggested that Kallistatin was a new link between AD and diabetes.

287 A hallmark of AD is the aggregation of Aβ into amyloid plaques and tau
288 phosphorylation in patients' brains. Aβ, a small peptide with a high propensity to form
289 aggregates, is widely believed to be central and initial to the pathogenesis of the
290 disease [61]. Correspondingly, we discovered Kallistatin could lead to Aβ
291 overproduction through Notch1/HES1/PPARγ/BACE1 signaling pathway. GSK-3β, a

292 vital kinase regulating the process of tau phosphorylation [53], could be activated by
293 inhibiting the Wnt signaling pathway. Kallistatin was already promoted as a
294 competitive inhibitor of LRP6, the Wnt receptor [55]. Consistent with previous reports,
295 Kallistatin could increase tau phosphorylation by activating GSK-3β. We
296 demonstrated for the first time that Kallistatin could promote AD by increasing Aβ
297 production and tau phosphorylation in the central nervous system.

298 Previous studies have shown that Notch signaling is closely related to AD. For
299 example, NOTCH mutation was reported to cause AD-like pathology [62]. And Notch1
300 was found to increase in AD patients [63]. Besides, the Notch1/HES1 signaling pathway
301 was reported to suppress the expression of PPARγ [64]. Our previous studies proved that
302 Kallistatin could activate Notch1 signaling [37]. Consequently, we detect Notch1 in our
303 animal and cell models. Indeed, Notch1 was upregulated by Kallistatin (Fig.6, S4), as
304 well as Aβ deposition. Notch signaling is initiated by receptor-ligand interaction at the
305 cell surface. In mammals, there are five ligands encoded by JAG1, JAG2, DLL1,
306 DLL3, and DLL4 [65]. Here, our results found that Kallistatin could activate Notch1 by
307 binding to it directly, which means Kallistatin was a new ligand of the Notch1
308 receptor.

309 Treatment of AD has always been a hot and challenging problem in neurology.
310 Multiple strategies have been proposed to reduce the pathogenicity of Aβ and tau.
311 Unfortunately, several Aβ-targeted therapies tested in the phase III clinical trials have
312 failed as they have not been able to slow down cognitive decline, although they could

313 effectively reduce the Aβ load [66, 67, 68, 69, 70, 71]. BACE1 inhibitors were failed to
314 improve the cognitive function of AD patients but also resulted in clinical
315 deterioration and impairment of liver function [72, 73, 74]. Here are two possible reasons
316 for the failure of of clinical trials with the BACE1 inhibitor. First, the reduction of
317 BACE1 activity could lead to an accumulation of full-length APP [75]. Second, the size
318 of the BACE1 active site is relatively large; the use of a small molecule may not be
319 sufficient to occupy the active site [76]. Therefore, synaptic damage caused by BACE1
320 inhibitors or the insufficient effect of BACE1 inhibitors may lead to the failure of
321 clinical trials. Therapeutic strategies targeting tau include tau aggregation blockers
322 (TRx0014, TRx0237), antibody vaccine therapy (e.g., RO7105705, BIIB092),
323 inhibition of tau phosphorylation (Anavex2-73), and microtubule stabilizers
324 (Anavex2-73) [77]. Some of the aforementioned drugs have been partially stopped,
325 while others are still undergoing a clinical test and shown protective benefits. There
326 are still several obstacles to the commercialization of tau treatments when they reach
327 maturity.

328 Because of the failures of clinical trials, some researchers propose an alternative
329 option for AD therapeutics to address the modifiable risk factors for developing AD,
330 such as type 2 diabetes [78, 79, 80]. Our previous study proved that Kallistatin is a
331 multifunctional protein strongly associated with diabetes, and Kallistatin neutralizing
332 antibody improves diabetic wound healing [44]. This study demonstrated that Kallistatin
333 induced memory cognitive dysfunction by promoting Aβ deposition and tau

334 phosphorylation. Thus, we speculate the increased Kallistatin is a decent candidate for
335 T2DM-related AD therapy. PPARγ is a ligand-activated transcription factor and a
336 master modulator of glucose and lipid metabolism, organelle differentiation, and
337 inflammation [81, 82]. Growing evidence revealed that PPARγ agonists (rosiglitazone)
338 could rescue memory impairment of AD model mice [83, 84, 85]. In clinical trials, it is
339 controversial whether rosiglitazone has a protective effect on memory cognitive
340 function [86, 87, 88]. In this study, although Aβ expression had a downward trend, the
341 memory and cognition of KAL-TG mice were unchanged after treatment with
342 rosiglitazone for a month (Fig.8). This might be caused by insufficient treatment time
343 and the unchanged Kallistatin level.

344 Fenofibrate is a fibric acid derivative for clinically lowering blood lipids, mainly
345 triglycerides [89]. Studies showed that fenofibrate could prevent memory disturbances,
346 maintain hippocampal neurogenesis, and protect against Parkinson's disease (PD) [90,
347 91]. Specifically, fenofibrate has a neuroprotective effect on memory impairment
348 induced by Aβ through targeting α- and β- secretase [92]. Recently, our study proved
349 that the fenofibrate could repair the disrupted glutamine-glutamate cycle by
350 upregulating glutamine synthetase, while there is currently no fenofibrate treatment of
351 AD in clinical trials[38]. In this study, we proved fenofibrate was beneficial for memory
352 and cognitive impairment of KAL-TG mice. In addition, Aβ, BACE1, phosphorylated
353 tau and serum Kallistatin level of KAL-TG mice could be downregulated after the
354 treatment of fenofibrate. All of these suggested that fenofibrate might be helpful for

355 metabolic abnormalities-related AD patients. Therefore, fenofibrate administration in
356 patients with metabolic syndrome play an early role in preventing and treating AD.
357 In summary, we affirmed that Kallistatin concentrations were increased in
358 diabetes-related AD patients. In addition, our study demonstrated for the first time that
359 Kallistatin positively regulated Aβ42 through Notch1/HES1/PPARγ/BACE1, and
360 increased phosphorylated tau through inhibition of the Wnt signaling pathway.
361 Kallistatin might play a crucial role in linking diabetes and cognitive memory
362 deterioration. Moreover, fenofibrate could decrease the serum Kallistatin level,
363 BACE1, Aβ, and phosphorylated tau of KAL-TG mice, leading to alleviating memory
364 and cognitive impairment. These findings might provide new insight into AD and
365 possibly other neurodegenerative disorders.
366

367 **Materials and methods**

368 **Ethics approval and consent to participate**

369 All patients involved in this study gave their informed consent. This study
370 obtained the institutional review board approval of Medical Ethics of Zhongshan
371 Medical College No. 072 in 2021 and Animal Experiment Ethics of Zhongshan
372 Medical College, Approval No.: SYSU-IACUC-2019-B051.

373 **Human Subjects**

374 The study was approved by the experimental ethics committee of Guangdong
375 Academy of Medical Sciences and Sun Yat-sen University and carried out in strict

376 accordance with the ethical principles, and each participant was provided written
377 informed consent before collecting samples. We certify that the study was performed
378 in accordance with the 1964 declaration of HELSINKI and later amendments. We
379 collected 61 normal human samples, 56 AD patient samples, of whom 36 normal
380 human samples were from the Zhongshan City People's Hospital; 14 normal human
381 samples and 22 AD patient samples were from Zhongshan Third People's Hospital;
382 11 normal human samples and 14 AD patient samples were from Sun Yat-sen
383 Memorial Hospital. AD patient was clinically diagnosed according to ICD-10
384 (International Classification of Diseases) and NINCDS-ADRDA (the National
385 Institute of Neurological and Communicative Disorders and Stroke and the
386 Alzheimer's Disease and Related Disorders Association) criteria, and 20 AD patient
387 samples were clinically diagnosed according to MMSE (Mini-Mental State
388 Examination), were collected from Guangdong Provincial People's Hospital. All
389 subjects' Clinical characteristics were presented in Supplementary Tables (Table S1-
390 2).

391 **Experimental Animals and Protocols**

392 All animal experiment procedures were carried out in an environment without
393 specific pathogens (Specific pathogen free, SPF) with the approval of the Animal
394 Care and Use Committee of Sun Yat-sen University (approval ID: SYXK 2015-0107).
395 The wild type mice (WT, C57BL/6) were purchased from the Animal Center of
396 Guangdong Province (Production license No.: SCXK 2013-0002, Guangzhou, China).

397 The SAMR1 and SAMP8 mice (7 months old) were purchased from Tianjin
398 University of Traditional Chinese Medicine (Tianjin, China). Kallistatin transgenic
399 mice (KAL-TG) were C57BL/6 strain provided by Dr. Jianxing Ma (University of
400 Oklahoma Health Sciences Center) [39]. The KAL-TG mice genotype was identified by
401 PCR technology (forward primer: 5'-AGGGAAG-ATTGTGGATTTGG-3', reverse
402 primer: 5'-ATGAAGATACCAGTGATGCTC-3'). KAL-TG mice aged 6 months were
403 randomly divided into three groups: control group (KAL-TG), fenofibrate-treated
404 group (KAL-TG-Feno, 0.3 g/kg/d), and rosiglitazone-treated group (KAL-TG-RSG,
405 0.005 g/kg/d). Fenofibrate (Sigma-Aldrich, cat. no. F6020) and rosiglitazone
406 (Selleck, cat. no. S2556) were administered to mice by oral gavage. In three groups,
407 the serum Kallistatin were examined in the 0 week and 4 week after drug treatment
408 from the blood taken from mouse orbit. In addition, the Morris water maze and Y-
409 maze test were performed one week after the second blood collection.

410 **Morris water maze (MWM)**

411 The KAL-TG and WT mice were employed for the Morris water maze test
412 including the behavioral test, latency experiment (for 6 days), and the probe test (the
413 7th day). In addition, the MWM was performed as described previously [40]. Mice were
414 brought into the testing room and handled for 1 day before the training experiment. In
415 the 6-day training experiment, each mouse was trained with four daily trials. The mice
416 facing the wall were placed into the maze, exploring the maze from different
417 directions (east, south, west, and north). This trial was completed as soon as the

418 mouse found the platform, or 90 s elapsed. If the mice could discover and climb the
419 submerged platform within 90 s, the system would automatically record the latency
420 time and path immediately, and then the mouse was guided to and placed on the
421 submerged platform for extra 20 s. On day 7, the platform was removed, and a probe
422 test was performed to examine the strength and integrity of the animal spatial memory
423 24 h after the last testing trial. During the probe test, the mice were gently brought
424 into the water from the fixed monitoring point, and the mice were allowed to swim for
425 90 s without the platform. Finally, all of the measured behavioral parameters were
426 analyzed using SMART software.

427 **Y-maze test**

428 A Y maze test was performed to assess the mice's spatial memory. The Y maze
429 was separated by 120°, consisting of three identical arms (30 cm long, 7 cm wide, and
430 15 cm high) made of blue PVC. The mice were placed first in one of the arms, and
431 over the next 10 minutes, the sequence and number of their entry into the three arms
432 were monitored. An alternation is defined when a mouse visits three straight arms
433 (namely, ABC, BCA, or CAB, but not ABA, BAB, or CAC). Spontaneous alternation
434 (%) = [(number of alternations)/(total number of arms−2)]× 100.

435 **Electrophysiology**

436 Hippocampal slices (300-400 μm) from KAL-TG and WT mice were cut as
437 described [41]. Coronal slices from hippocampus (400 μm thick) were prepared from
438 different age groups KAL-TG mice and their WT littermates using a tissue slicer

439 (Vibratome 3000; Vibratome) in ice-cold dissection buffer containing the following
440 (in mM): 212.7 sucrose, 3 KCl, 1.25 NaH_2PO_4, 3 $MgCl_2$, 1 $CaCl_2$, 26 $NaHCO_3$, and
441 10 dextrose, bubbled with 95% O_2/5% CO_2. The slices were immediately transferred
442 to ACSF at 35 °C for 30 min before recordings. The recipe of ACSF was similar to the
443 dissection buffer, except that sucrose was replaced with 124 mM NaCl, and the
444 concentrations of $MgCl_2$ and $CaCl_2$ were changed to 1 mM and 2 mM, respectively.
445 All recordings were performed at 28-30 °C. Pyramidal cells in CA1 areas were
446 identified visually under infrared differential interference contrast optics based on
447 their pyramidal somata and prominent apical dendrites. Whole-cell was performed
448 using an Integrated Patch-Clamp Amplifier (Sutter Instrument, Novato, CA, USA)
449 controlled by Igor 7 software (WaveMetrics, Portland, OR, USA) filtered at 5 kHz and
450 sampled at 20 kHz. Igor 7 software was also used for acquisition and analysis. Only
451 cells with series resistance <20 MΩ and input resistance >100 MΩ were studied. Cells
452 were excluded if input resistance changed >15% or series resistance changed >10%
453 over the experiment. A concentric bipolar stimulating electrode with a tip diameter of
454 125 μm (FHC) was placed in the stratum radiatum. The recording and stimulating
455 electrode distances were kept at 50-100 μm. Patch pipettes (2-4MΩ) were filled with
456 the internal solution consisting of the following (in mM): 120 Cs-methylsulfonate, 10
457 Na-phosphocreatine, 10 HEPES, 4 ATP, 5 lidocaine N-ethyl bromide (QX-314), 0.5
458 GTP; the pH of the solution was 7.2–7.3, and the osmolarity was 270-285 mOsm.

459 To induce LTP, a pairing protocol was applied. In brief, conditioning stimulation
460 consisted of 360 pulses at 2 Hz paired with continuous postsynaptic depolarization
461 (180 s) to 0 mV. 50 μM picrotoxin was added to the recording bath to suppress
462 excessive polysynaptic activity, and the concentration of Ca^{2+} and Mg^{2+} was elevated
463 to 4 mM to reduce the recruitment of polysynaptic responses. A test pulse was
464 delivered at 0.067 Hz to monitor baseline amplitude for 10 min before and 30 min
465 following paired stimulation. To calculate LTP, the EPSC amplitude was normalized
466 to the mean baseline amplitude during 10 min baseline. Potentiation was defined as
467 the mean normalized EPSC amplitude 25–40 min after paired stimulation.

468 **ELISA**

469 To quantify serum Kallistatin, the collected samples were centrifuged at 4 °C for
470 10min at 5000 rpm. It was detected using the KBP ELISA kit (#DY1669, R&D
471 systems, MN, USA) as per the instructions of the manufacturer. The levels of Aβ42 in
472 brain tissue produced from mouse primary neuron cells and HT22 cells were
473 measured with a mouse Aβ42 Elisa Kit (27721, IBL, Germany). To measure Aβ42 in
474 brain tissue, 0.05 g of mouse brain tissues were weighed and homogenized using 2ml
475 PBS with a protease inhibitor (cocktail). After centrifugalization at 4 °C for 30 min at
476 12000 g, the extracts' supernatants were analyzed using the ELISA method after total
477 protein quantification. To quantify levels of Aβ42 produced from primary neuron
478 cells, the cell supernatants were ultrafiltrated with an Ultrafiltration tube (4-kD
479 Millipore), centrifugalization, and testing. Cell homogenate was prepared in 1ml PBS

480 with a protease inhibitor (cocktail) and quantified using the BCA method before being
481 measured by ELISA.

482 **Immunohistochemistry**

483 Tissue slices were prepared as described before [42]. The sections were incubated
484 with Aβ (ab201060, Abcam, Cambridge, UK), BACE1 (#5606S, Cell Signaling
485 Technology, Boston, USA), PPARγ (#2435, Cell Signaling Technology, Boston,
486 USA), Notch1 (#3608, Cell Signaling Technology, Boston, USA), p-tau S202
487 (ab108387, Abcam, Cambridge, UK), p-tau T231(ab151559, Abcam, Cambridge,
488 UK), p-tau S396 (ab109390, Abcam, Cambridge, UK), tau (ab75714, Abcam,
489 Cambridge, UK) antibodies overnight at 4°C and then incubated with Alexa Fluor
490 488-donkey anti-rabbit IgG (H + L) (1:200, Life Technologies, Gaithersburg, MD,
491 USA, #A21208) for 1h, then incubated with a biotin-conjugated secondary antibody
492 for 30 min, followed by incubation with DAB for 10 s and hematoxylin staining for
493 30 s. The IHC signals were analyzed using ImageJ.

494 **Cell culture experiments**

495 HT22 cells were purchased from the Cell Bank of the Chinese Academy of
496 Sciences (Shanghai, China). HT22 cells were cultured and grown to confluence in
497 DMEM supplemented with 10% FBS (Gibco BRL), 100 U/mL penicillin, and 100
498 U/mL streptomycins (Gibco BRL).

499 **Primary culture of hippocampal neurons**

500 Primary neurons were obtained from the hippocampus of C57/BL6J mice at age
501 1-3 days. Before culturing, the newborn pup was euthanized and dipped into 70%

502 ethanol for 3 min. First, the infant pup hippocampus was isolated with eye tweezers
503 observed under the stereomicroscope, and excess soft tissue was removed. Second,
504 hippocampal tissue in PBS buffer was cut up with scissors gently and blown with a
505 1ml pipette until it was not visible. Next, the cell suspension was transferred to a 15ml
506 centrifuge tube and centrifuged at 1000 rpm for 5 min at room temperature. Cell
507 precipitation was suspended and cultured with 2-3mL primary neural stem cell (NSC)
508 suspension (Thermo Fisher Scientific, 21103049) in a 37 °C, 5% CO_2 cell incubator
509 for 3 days, changing half medium every 2 days. After 7 days, the cell suspension was
510 transferred to a 15ml centrifuge tube, centrifuged, and recultured with neurobasal,
511 10%FBS, 1:50 B27(Thermo Fisher Scientific, A3582801), and 1:100 bFGF (Thermo
512 Fisher Scientific, #RP-8626). One day later, the medium was changed to neurobasal
513 (2%FBS, 1:50 B27, and 1:100 bFGF), culturing for 21 more days. The
514 immunofluorescence technique was used with the neuron-specific marker (MAP2,
515 #4542, Cell Signaling Technology, Boston, USA) to determine the purity of neurons.

516 **siRNA, shRNA, and adenovirus transfection**

517 Notch1 siRNA and control siRNA were purchased from RiboBio (Guangzhou,
518 China). HES1 shRNA and control shRNA were purchased from Qingke (Guangzhou,
519 China). Green fluorescent protein-adenovirus (Ad-GFP) and Kallistatin-adenovirus
520 (Ad-KAL) were provided by Dr. Jianxing Ma (University of Oklahoma Health
521 Sciences Center). According to the manufacturer's instructions, the transfections were
522 performed at approximately 60% confluency using Lipofectamine®3000 transfection

523 reagent (Invitrogen) or RNAiMAX. After 24 h, interference confirmation was
524 conducted using real-time quantitative PCR (RT-qPCR) and Western blot.

525 **RNA isolation and quantitative RT-PCR**

526 Total RNA extraction, reverse transcription of cDNA, and real-time quantitative
527 PCR were performed as described previously [43]. BACE1 forward:
528 GGAGCCCTTCTTTGACTCCC; BACE1 reverse:
529 CAATGATCATGCTCCCTCCCA; ADAM9 forward:
530 GGAAGGCTCCCTACTCTCTGA; ADAM9 reverse: CAATTCC-
531 AAAACTGGCATTCTCC; ADAM10 forward: ATGGTGTTGCCGACAGTGTTA;
532 ADAM10 reverse: GTTTGGCACGCTGGTGTTTTT; ADAM17 forward: GGAT-
533 CTACAGTCTGCGACACA; ADAM17 reverse:
534 TGAAAAGCGTTCGGTACTTGAT; β-actin forward:
535 GCACTCTTCCAGCTTCCTT; β-actin reverse: GTTGGCGTACAG-GTCTTTGC.

536 **Western blot**

537 Western blot was performed as described previously [40, 43]. Equal amounts of
538 protein were subjected to western blot analysis. Blots were probed with antibodies
539 against Kallistatin (ab187656, Abcam, Cambridge, UK), Aβ (ab201060, Abcam,
540 Cambridge, UK), Presenilin-1 (ab76083, Abcam, Cambridge, UK), BACE1 (#5606S,
541 Cell Signaling Technology, Boston, USA), APP (#2452S, Cell Signaling Technology,
542 Boston, USA), MAP2 (#4542, Cell Signaling Technology, Boston, USA), PPARγ
543 （#2435, Cell Signaling Technology, Boston, USA), SP1 (#9389, Cell Signaling

544 Technology, Boston, USA), YY1 (#46395, Cell Signaling Technology, Boston,
545 USA）, Notch1 (#3608, Cell Signaling Technology, Boston, USA), Hes1 (#11988,
546 Cell Signaling Technology, Boston, USA), p-tau S202 (ab108387, Abcam,
547 Cambridge, UK), p-tau T231(ab151559, Abcam, Cambridge, UK), p-tau S396
548 (ab109390, Abcam, Cambridge, UK), tau (ab75714, Abcam, Cambridge, UK),
549 GSK3β(#70109S, Cell Signaling Technology, Boston, USA), p-GSK3β Ser9 (#9323,
550 Cell Signaling Technology, Boston, USA), β-actin (A5441-2ml, Sigma, CA, USA),
551 anti-Mouse (#PI200, Vector Laboratories, Burlingame, CA, USA), anti-Rabbit
552 (#PI1000, Vector Laboratories, Burlingame, CA, USA). The signal intensity was
553 quantified using ImageJ (NIH).

554 **Statistical Analysis**

555 The results are expressed as mean ± SD. Student's *t*-test was applied for
556 comparisons of parametric data between two groups, and one-way ANOVA followed
557 by LSD *t*-test was used to compare differences between more than two different
558 groups (GraphPad Prism software). A *P* value less than 0.05 was considered statistical
559 significance.

560 **List of abbreviations**

Aβ	amyloid β
p-tau	hyperphosphorylated tau
AD	Alzheimer's disease
T2DM	type 2 diabetes mellitus

FBG	fasting blood glucose
TG	triglyceride
KAL-TG	Kallistatin-transgenic
WT	wild type mice
APP	amyloid precursor protein
BACE1	β-site APP cleaving enzyme 1
BMI	body mass index
ICD-10	The International Statistical Classification of Diseases and Related Health Problems 10th Revision
NINCDS-ADRDA	the National Institute of Neurological and Communicative Disorders and Stroke and the Alzheimer's Disease and Related Disorders Association
MMSE	mini-Mental State Examination
KAL-TG-RSG	rosiglitazone-treated group
KAL-TG-Feno	fenofibrate-treated group
MWM	morris water maze
RT-qPCR	real-time quantitative PCR

Declarations

Ethics approval and consent to participate

All patients involved in this study gave their informed consent. This study obtained the institutional review board approval of Medical Ethics of Zhongshan Medical College No. 072 in 2021 and Animal Experiment Ethics of Zhongshan Medical College, Approval No.: SYSU-IACUC-2019-B051.

Consent for publication

Not applicable.

Availability of data and materials

All the data supporting the conclusions of the current study are presented in the figures and they are available from the corresponding authors upon reasonable request. There are no restrictions on data availability. Source data are provided with this paper.

Competing interests

The authors declare that they have no competing interests.

Acknowledgements

We are thankful to Zhongshan City People's Hospital, Zhongshan Third People's Hospital, Guangdong Provincial People's Hospital, and Sun Yat-sen Memorial Hospital for kindly providing serum samples for the analyses of this manuscript. We thank Professor Boxing Li for his valuable advice on our study.

Funding

This study was supported by The National Natural Science Foundation of China (Grants 82070888, 82070882, 82100917, 82273116, 82203661, 81901557, 81870869, and 32071101); Guangdong Natural Science Fund (Grant 2022A1515012423, 2021A1515010434, 2023A1515010316, and 2023A1515010214); Key Sci-Tech Research Project of Guangzhou Municipality, China (Grants 202201010820, 202102020955); Key Project of Nature Science Foundation of Guangdong Province,

China (Grant 2019B1515120077); National Key R&D Program of China (Grant 2018YFA0800403); Guangdong Special Support Program for Young Top Scientist (Grant 201629046); China Postdoctoral Science Foundation (Grant 2021M703679, 2022M713594, BX20220360); Health Commission of Guangdong Province (Grants A2022161) ; Guangzhou Municipal Science and Technology Bureau (Grants SL2022A04J01575); Guangdong Key Project in "Development of new tools for diagnosis and treatment of Autism" (2018B030335001), Research and Development Plan of Key Areas of Guangzhou Science and Technology Bureau (2020070030001), Open Research Funds of State Key Laboratory of Ophthalmology (2020KF03); Guangzhou Key Laboratory for Metabolic Diseases(202102100004); The Science and Technology Planning Project of Guangdong Province 2023B1212060018.

References

1. Grundke-Iqbal I, Iqbal K, Tung YC, Quinlan M, Wisniewski HM, Binder LI. Abnormal phosphorylation of the microtubule-associated protein tau (tau) in Alzheimer cytoskeletal pathology. *Proceedings of the National Academy of Sciences of the United States of America* 1986, **83**(13)**:** 4913-4917.

2. Haass C, Selkoe DJ. Soluble protein oligomers in neurodegeneration: lessons from the Alzheimer's amyloid beta-peptide. *Nature Reviews Molecular Cell Biology* 2007, **8**(2)**:** 101-112.

3. Holtzman DM, Morris JC, Goate AM. Alzheimer's Disease: The Challenge of the Second Century. *Science Translational Medicine* 2011, **3**(77).

4. Leng F, Edison P. Neuroinflammation and microglial activation in Alzheimer disease: where do we go from here? *Nature Reviews Neurology* 2021, **17**(3)**:** 157-172.

5. De Strooper B, Karran E. The Cellular Phase of Alzheimer's Disease. *Cell* 2016, **164**(4)**:** 603-615.

6. Tomita T. Molecular mechanism of intramembrane proteolysis by gamma-secretase. *Journal of Biochemistry* 2014, **156**(4)**:** 195-201.

7. LaFerla FM, Green KN, Oddo S. Intracellular amyloid-beta in Alzheimer's disease. *Nature Reviews Neuroscience* 2007, **8**(7)**:** 499-509.

8. Das B, Yan R. A Close Look at BACE1 Inhibitors for Alzheimer's Disease Treatment. *Cns Drugs* 2019, **33**(3)**:** 251-263.

9. Crunkhorn, Sarah. Alzheimer disease: BACE1 inhibitor reduces β-amyloid production in humans. *Nature Reviews Drug Discovery* 2016, **16**(1)**:** 18-18.

10. Yan R, Vassar R. Targeting the β secretase BACE1 for Alzheimer's disease therapy. *Lancet Neurology* 2014, **13**(3)**:** 319-329.

11. Wang Y, Mandelkow E. Tau in physiology and pathology. *Nature reviews Neuroscience* 2016, **17**(1)**:** 5-21.

12. Hausrat TJ, Janiesch PC, Breiden P, Lutz D, Hoffmeister-Ullerich S, Hermans-Borgmeyer I*, et al.* Disruption of tubulin-alpha4a polyglutamylation prevents aggregation of hyper-phosphorylated tau and microglia activation in mice. *Nature communications* 2022, **13**(1)**:** 4192.

13. Braak E, Braak H, Mandelkow EM. A sequence of cytoskeleton changes related to the formation of neurofibrillary tangles and neuropil threads. *Acta neuropathologica* 1994, **87**(6)**:** 554-567.

14. Boonen RA, van Tijn P, Zivkovic D. Wnt signaling in Alzheimer's disease: up or down, that is the question. *Ageing Res Rev* 2009, **8**(2)**:** 71-82.

15. Biessels GJ, Despa F. Cognitive decline and dementia in diabetes mellitus: mechanisms and clinical implications. *Nature Reviews Endocrinology* 2018, **14**(10)**:** 591-604.

16. Li W, Huang E, Gao S. Type 1 Diabetes Mellitus and Cognitive Impairments: A Systematic Review. *Journal of Alzheimers Disease* 2017, **57**(1)**:** 29-36.

17. Cardoso SM, Correia SC, Carvalho C, Moreira PI. Mitochondria in Alzheimer's Disease and Diabetes-Associated Neurodegeneration: License to Heal! In: Singh H, Sheu SS (eds). *Pharmacology of Mitochondria*, vol. 240, 2017, pp 281-308.

18. Schipper HM. Apolipoprotein E: Implications for AD neurobiology, epidemiology and risk assessment. *Neurobiology of Aging* 2011, **32**(5)**:** 778-790.

19. Folch J, Patraca I, Martinez N, Pedros I, Petrov D, Ettcheto M*, et al.* The role of leptin in the

sporadic form of Alzheimer's disease. Interactions with the adipokines amylin, ghrelin and the pituitary hormone prolactin. *Life Sciences* 2015, **140:** 19-28.

20. Association As. 2016 Alzheimer's disease facts and figures. *Alzheimer's & Dementia* 2016, **12**(4)**:** 459-509.

21. Baglietto-Vargas D, Shi J, Yaeger DM, Ager R, LaFerla FM. Diabetes and Alzheimer's disease crosstalk. *Neuroscience & Biobehavioral Reviews* 2016, **64:** 272-287.

22. Kandimalla R, Thirumala V, Reddy PH. Is Alzheimer's disease a Type 3 Diabetes? A critical appraisal. *Biochimica Et Biophysica Acta-Molecular Basis of Disease* 2017, **1863**(5)**:** 1078-1089.

23. Zhang Y, Huang N-q, Yan F, Jin H, Zhou S-y, Shi J-s*, et al.* Diabetes mellitus and Alzheimer's disease: GSK-3 beta as a potential link. *Behavioural Brain Research* 2018, **339:** 57-65.

24. Steen E, Terry BM, Rivera EJ, Cannon JL, Neely TR, Tavares R*, et al.* Impaired insulin and insulin-like growth factor expression and signaling mechanisms in Alzheimer's disease - is this type 3 diabetes? *Journal of Alzheimers Disease* 2005, **7**(1)**:** 63-80.

25. Candasamy M, Mohamed Elhassan SA, Kumar Bhattamisra S, Hua WY, Sern LM, Binti Busthamin NA*, et al.* Type 3 diabetes (Alzheimer's disease): new insight for promising therapeutic avenues. *Panminerva Medica* 2020, **62**(3)**:** 155-163.

26. Koekkoek PS, Kappelle LJ, van den Berg E, Rutten GE, Biessels GJ. Cognitive function in patients with diabetes mellitus: guidance for daily care. *The Lancet Neurology* 2015, **14**(3)**:** 329-340.

27. Hildreth KL, Van Pelt RE, Schwartz RS. Obesity, insulin resistance, and Alzheimer's disease. *Obesity (Silver Spring, Md)* 2012, **20**(8)**:** 1549.

28. Anjum I, Fayyaz M, Wajid A, Sohail W, Ali A. Does obesity increase the risk of dementia: a literature review. *Cureus* 2018, **10**(5).

29. Ma C, Luo C, Yin H, Zhang Y, Xiong W, Zhang T*, et al.* Kallistatin inhibits lymphangiogenesis and lymphatic metastasis of gastric cancer by downregulating VEGF-C expression and secretion. *Gastric Cancer* 2018, **21**(4)**:** 617-631.

30. Yang Y, He X, Cheng R, Chen Q, Shan C, Chen L*, et al.* Diabetes-induced upregulation of kallistatin levels exacerbates diabetic nephropathy via RAS activation. *Faseb Journal* 2020, **34**(6)**:** 8428-8441.

31. Ma C, Yin H, Zhong J, Zhang Y, Luo C, Che D*, et al.* Kallistatin exerts anti-lymphangiogenic effects by inhibiting lymphatic endothelial cell proliferation, migration and tube formation.

International Journal of Oncology 2017, **50**(6)**:** 2000-2010.

32. El-Asrar MA, Andrawes NG, Ismail EA, Salem SMH. Kallistatin as a marker of microvascular complications in children and adolescents with type 1 diabetes mellitus: Relation to carotid intima media thickness. *Vascular Medicine* 2015, **20**(6)**:** 509-517.

33. Gateva A, Assyov Y, Velikova T, Kamenov Z. Increased kallistatin levels in patients with obesity and prediabetes compared to normal glucose tolerance. *Endocrine Research* 2017, **42**(2)**:** 163-168.

34. Campbell DJ, Kladis A, Zhang Y, Jenkins AJ, Prior DL, Yii M*, et al.* Increased tissue kallikrein levels in type 2 diabetes. *Diabetologia* 2010, **53**(4)**:** 779-785.

35. Nowicki GJ, Ślusarska B, Polak M, Naylor K, Kocki T. Relationship between Serum Kallistatin and Afamin and Anthropometric Factors Associated with Obesity and of Being Overweight in Patients after Myocardial Infarction and without Myocardial Infarction. *Journal of clinical medicine* 2021, **10**(24).

36. Hong S, Han K, Park CY. The insulin resistance by triglyceride glucose index and risk for dementia: population-based study. *Alzheimer's research & therapy* 2021, **13**(1)**:** 9.

37. Feng J, Dong C, Long YL, Mai LF, Ren M, Li LY*, et al.* Elevated Kallikrein-binding protein in diabetes impairs wound healing through inducing macrophage M1 polarization. *Cell Communication and Signaling* 2019, **17**.

38. Long Y, Zhao Z, Xie W, Shi J, Yang F, Zhu D*, et al.* Kallistatin leads to cognition impairment via downregulating glutamine synthetase. *Pharmacol Res* 2024, **202:** 107145.

39. McBride JD, Jenkins AJ, Liu XC, Zhang B, Lee K, Berry WL*, et al.* Elevated Circulation Levels of an Antiangiogenic SERPIN in Patients with Diabetic Microvascular Complications Impair Wound Healing through Suppression of Wnt Signaling. *Journal of Investigative Dermatology* 2014, **134**(6)**:** 1725-1734.

40. Huang M, Qi WW, Fang SH, Jiang P, Yang C, Mo YS*, et al.* Pigment Epithelium-Derived Factor Plays a Role in Alzheimer's Disease by Negatively Regulating A beta 42. *Neurotherapeutics* 2018, **15**(3)**:** 728-741.

41. Guo D, Peng Y, Wang L, Sun X, Wang X, Liang C*, et al.* Autism-like social deficit generated by Dock4 deficiency is rescued by restoration of Rac1 activity and NMDA receptor function. *Mol Psychiatry* 2021, **26**(5)**:** 1505-1519.

42. Li C, Huang Z, Zhu L, Yu X, Gao T, Feng J*, et al.* The contrary intracellular and extracellular functions of PEDF in HCC development. *Cell Death & Disease* 2019, **10**.

43. Jiang P, Huang M, Qi WW, Wang FH, Yang TY, Gao TX, *et al.* FUBP1 promotes neuroblastoma proliferation via enhancing glycolysis-a new possible marker of malignancy for neuroblastoma. *Journal of Experimental & Clinical Cancer Research* 2019, **38**(1).

44. Feng J, Dong C, Long Y, Mai L, Ren M, Li L, *et al.* Elevated Kallikrein-binding protein in diabetes impairs wound healing through inducing macrophage M1 polarization. *Cell Communication and Signaling* 2019, **17**.

45. De Strooper B, Annaert W. Proteolytic processing and cell biological functions of the amyloid precursor protein. *Journal of Cell Science* 2000, **113**(11)**:** 1857-1870.

46. LaFerla FM, Oddo S. Alzheimer's disease: A beta, tau and synaptic dysfunction. *Trends in Molecular Medicine* 2005, **11**(4)**:** 170-176.

47. Scheuner D, Eckman C, Jensen M, Song X, Citron M, Suzuki N, *et al.* Secreted amyloid beta-protein similar to that in the senile plaques of Alzheimer's disease is increased in vivo by the presenilin 1 and 2 and APP mutations linked to familial Alzheimer's disease. *Nature Medicine* 1996, **2**(8)**:** 864-870.

48. Christensen MA, Zhou WH, Qing H, Lehman A, Philipsen S, Song WH. Transcriptional regulation of BACE1, the beta-amyloid precursor protein beta-secretase, by Sp1. *Molecular and Cellular Biology* 2004, **24**(2)**:** 865-874.

49. Lin N, Chen L-m, Pan X-d, Zhu Y-g, Zhang J, Shi Y-q, *et al.* Tripchlorolide Attenuates beta-amyloid Generation via Suppressing PPAR gamma-Regulated BACE1 Activity in N2a/APP695 Cells. *Molecular Neurobiology* 2016, **53**(9)**:** 6397-6406.

50. Nowak K, Lange-Dohna C, Zeitschel U, Gunther A, Luscher B, Robitzki A, *et al.* The transcription factor Yin Yang 1 is an activator of BACE1 expression. *Journal of Neurochemistry* 2006, **96**(6)**:** 1696-1707.

51. Maniati E, Bossard M, Cook N, Candido JB, Emami-Shahri N, Nedospasov SA, *et al.* Crosstalk between the canonical NF-κB and Notch signaling pathways inhibits Pparγ expression and promotes pancreatic cancer progression in mice. *The Journal of clinical investigation* 2011, **121**(12)**:** 4685-4699.

52. Herzig S, Hedrick S, Morantte I, Koo SH, Galimi F, Montminy M. CREB controls hepatic lipid metabolism through nuclear hormone receptor PPAR-gamma. *Nature* 2003, **426**(6963)**:** 190-193.

53. Kanno T, Tsuchiya A, Tanaka A, Nishizaki T. Combination of PKCε Activation and PTP1B Inhibition Effectively Suppresses Aβ-Induced GSK-3β Activation and Tau Phosphorylation. *Mol*

Neurobiol 2016, **53**(7)**:** 4787-4797.

54. Piao S, Lee SH, Kim H, Yum S, Stamos JL, Xu Y*, et al.* Direct inhibition of GSK3beta by the phosphorylated cytoplasmic domain of LRP6 in Wnt/beta-catenin signaling. *PLoS One* 2008, **3**(12)**:** e4046.

55. Liu X, Zhang B, McBride JD, Zhou K, Lee K, Zhou Y*, et al.* Antiangiogenic and antineuroinflammatory effects of kallistatin through interactions with the canonical Wnt pathway. *Diabetes* 2013, **62**(12)**:** 4228-4238.

56. Kubis-Kubiak A, Wiatrak B, Piwowar A. Hyper-glycemia and insulinemia induce morphological changes and modulate secretion of S100B, S100A8, amyloid β 1-40 and amyloid β 1-42, in a model of human dopaminergic neurons. *Biomedicine & pharmacotherapy = Biomedecine & pharmacotherapie* 2022, **156:** 113869.

57. Rivas-Domínguez A, Mohamed-Mohamed H, Jimenez-Palomares M, García-Morales V, Martinez-Lopez L, Orta ML*, et al.* Metabolic Disturbance of High-Saturated Fatty Acid Diet in Cognitive Preservation. *International journal of molecular sciences* 2023, **24**(9).

58. Suzanne M. Type 3 diabetes is sporadic Alzheimer′ s disease: mini-review. *European Neuropsychopharmacology* 2014, **24**(12)**:** 1954-1960.

59. Biessels GJ, Reagan LP. Hippocampal insulin resistance and cognitive dysfunction. *Nature reviews Neuroscience* 2015, **16**(11)**:** 660-671.

60. Xu W, Caracciolo B, Wang HX, Winblad B, Bäckman L, Qiu C*, et al.* Accelerated progression from mild cognitive impairment to dementia in people with diabetes. *Diabetes* 2010, **59**(11)**:** 2928-2935.

61. Selkoe DJ. Toward a comprehensive theory for Alzheimer's disease - Hypothesis: Alzheimer's disease is caused by the cerebral accumulation and cytotoxicity of amyloid beta-protein. In: Khachaturian ZS, Mesulam MM (eds). *Alzheimers Disease: A Compendium of Current Theories*, vol. 924, 2000, pp 17-25.

62. Thijs V, Robberecht W, De Vos R, Sciot R. Coexistence of CADASIL and Alzheimer's disease. *Journal of Neurology Neurosurgery and Psychiatry* 2003, **74**(6)**:** 790-792.

63. Brai E, Raio NA, Alberi L. Notch1 hallmarks fibrillary depositions in sporadic Alzheimer's disease. *Acta Neuropathologica Communications* 2016, **4**.

64. Liu B, Wang D, Xiong T, Liu Y, Jing X, Du J*, et al.* Inhibition of Notch Signaling Promotes the Differentiation of Epicardial Progenitor Cells into Adipocytes. *Stem Cells Int* 2021, **2021:** 8859071.

65. D'Souza B, Meloty-Kapella L, Weinmaster G. CANONICAL AND NON-CANONICAL NOTCH LIGANDS. In: Kopan R (ed). *Notch Signaling*, vol. 92, 2010, pp 73-129.

66. Salloway S, Sperling R, Fox NC, Blennow K, Klunk W, Raskind M*, et al.* Two Phase 3 Trials of Bapineuzumab in Mild-to-Moderate Alzheimer's Disease. *New England Journal of Medicine* 2014, **370**(4)**:** 322-333.

67. Ostrowitzki S, Lasser RA, Dorflinger E, Scheltens P, Barkhof F, Nikolcheva T*, et al.* A phase III randomized trial of gantenerumab in prodromal Alzheimer's disease. *Alzheimers Research & Therapy* 2017, **9**.

68. Honig LS, Vellas B, Woodward M, Boada M, Bullock R, Borrie M*, et al.* Trial of Solanezumab for Mild Dementia Due to Alzheimer's Disease. *New England Journal of Medicine* 2018, **378**(4)**:** 321-330.

69. Henley D, Raghavan N, Sperling R, Aisen P, Raman R, Romano G. Preliminary Results of a Trial of Atabecestat in Preclinical Alzheimer's Disease. *New England Journal of Medicine* 2019, **380**(15)**:** 1483-1485.

70. Egan MF, Kost J, Voss T, Mukai Y, Aisen PS, Cummings JL*, et al.* Randomized Trial of Verubecestat for Prodromal Alzheimer's Disease. *New England Journal of Medicine* 2019, **380**(15)**:** 1408-1420.

71. Panza F, Lozupone M, Logroscino G, Imbimbo BP. A critical appraisal of amyloid-beta targeting therapies for Alzheimer disease. *Nature Reviews Neurology* 2019, **15**(2)**:** 73-88.

72. Wessels AM, Lines C, Stern RA, Kost J, Voss T, Mozley LH*, et al.* Cognitive outcomes in trials of two BACE inhibitors in Alzheimer's disease. *Alzheimer's & dementia : the journal of the Alzheimer's Association* 2020, **16**(11)**:** 1483-1492.

73. Novak G, Streffer JR, Timmers M, Henley D, Brashear HR, Bogert J*, et al.* Long-term safety and tolerability of atabecestat (JNJ-54861911), an oral BACE1 inhibitor, in early Alzheimer's disease spectrum patients: a randomized, double-blind, placebo-controlled study and a two-period extension study. *Alzheimers Res Ther* 2020, **12**(1)**:** 58.

74. Timmers M, Streffer JR, Russu A, Tominaga Y, Shimizu H, Shiraishi A*, et al.* Pharmacodynamics of atabecestat (JNJ-54861911), an oral BACE1 inhibitor in patients with early Alzheimer's disease: randomized, double-blind, placebo-controlled study. *Alzheimers Res Ther* 2018, **10**(1)**:** 85.

75. Nigam SM, Xu S, Ackermann F, Gregory JA, Lundkvist J, Lendahl U*, et al.* Endogenous APP accumulates in synapses after BACE1 inhibition. *Neuroscience research* 2016, **109:** 9-15.

76. Citron M. Emerging Alzheimer's disease therapies: inhibition of beta-secretase. *Neurobiol Aging* 2002, **23**(6)**:** 1017-1022.

77. Long JM, Holtzman DM. Alzheimer Disease: An Update on Pathobiology and Treatment Strategies. *Cell* 2019, **179**(2)**:** 312-339.

78. Livingston G, Sommerlad A, Orgeta V, Costafreda SG, Huntley J, Ames D*, et al.* Dementia prevention, intervention, and care. *Lancet* 2017, **390**(10113)**:** 2673-2734.

79. Butterfield DA, Di Domenico F, Barone E. Elevated risk of type 2 diabetes for development of Alzheimer disease: A key role for oxidative stress in brain. *Biochimica Et Biophysica Acta-Molecular Basis of Disease* 2014, **1842**(9)**:** 1693-1706.

80. Arnold SE, Arvanitakis Z, Macauley-Rambach SL, Koenig AM, Wang H-Y, Ahima RS*, et al.* Brain insulin resistance in type 2 diabetes and Alzheimer disease: concepts and conundrums. *Nature Reviews Neurology* 2018, **14**(3)**:** 168-181.

81. Zhao QY, Wu XH, Yan S, Xie XF, Fan YH, Zhang JQ*, et al.* The antidepressant-like effects of pioglitazone in a chronic mild stress mouse model are associated with PPAR gamma-mediated alteration of microglial activation phenotypes. *Journal of neuroinflammation* 2016, **13**.

82. Guo M, Li C, Lei Y, Xu S, Zhao D, Lu XY. Role of the adipose PPAR gamma-adiponectin axis in susceptibility to stress and depression/anxiety-related behaviors. *Molecular Psychiatry* 2017, **22**(7)**:** 1056-1068.

83. Toledo EM, Inestrosa NC. Activation of Wnt signaling by lithium and rosiglitazone reduced spatial memory impairment and neurodegeneration in brains of an APPswe/PSEN1DeltaE9 mouse model of Alzheimer's disease. *Mol Psychiatry* 2010, **15**(3)**:** 272-285, 228.

84. Escribano L, Simón AM, Gimeno E, Cuadrado-Tejedor M, López de Maturana R, García-Osta A*, et al.* Rosiglitazone rescues memory impairment in Alzheimer's transgenic mice: mechanisms involving a reduced amyloid and tau pathology. *Neuropsychopharmacology : official publication of the American College of Neuropsychopharmacology* 2010, **35**(7)**:** 1593-1604.

85. O'Reilly JA, Lynch M. Rosiglitazone improves spatial memory and decreases insoluble Aβ(1-42) in APP/PS1 mice. *Journal of neuroimmune pharmacology : the official journal of the Society on NeuroImmune Pharmacology* 2012, **7**(1)**:** 140-144.

86. Watson GS, Cholerton BA, Reger MA, Baker LD, Plymate SR, Asthana S*, et al.* Preserved cognition in patients with early Alzheimer disease and amnestic mild cognitive impairment during treatment with rosiglitazone: a preliminary study. *The American journal of geriatric psychiatry : official journal of the American Association for Geriatric Psychiatry* 2005, **13**(11)**:** 950-958.

87. Tzimopoulou S, Cunningham VJ, Nichols TE, Searle G, Bird NP, Mistry P, *et al.* A multi-center randomized proof-of-concept clinical trial applying [^{18}F]FDG-PET for evaluation of metabolic therapy with rosiglitazone XR in mild to moderate Alzheimer's disease. *Journal of Alzheimer's disease : JAD* 2010, **22**(4)**:** 1241-1256.

88. Harrington C, Sawchak S, Chiang C, Davies J, Donovan C, Saunders AM, *et al.* Rosiglitazone does not improve cognition or global function when used as adjunctive therapy to AChE inhibitors in mild-to-moderate Alzheimer's disease: two phase 3 studies. *Current Alzheimer research* 2011, **8**(5)**:** 592-606.

89. Keating GM, Croom KF. Fenofibrate: a review of its use in primary dyslipidaemia, the metabolic syndrome and type 2 diabetes mellitus. *Drugs* 2007, **67**(1)**:** 121-153.

90. Barbiero JK, Santiago R, Tonin FS, Boschen S, da Silva LM, Werner MF, *et al.* PPAR-α agonist fenofibrate protects against the damaging effects of MPTP in a rat model of Parkinson's disease. *Prog Neuropsychopharmacol Biol Psychiatry* 2014, **53:** 35-44.

91. Ouk T, Gautier S, Pétrault M, Montaigne D, Maréchal X, Masse I, *et al.* Effects of the PPAR-α agonist fenofibrate on acute and short-term consequences of brain ischemia. *Journal of Cerebral Blood Flow & Metabolism* 2014, **34**(3)**:** 542-551.

92. Assaf N, El-Shamarka ME, Salem NA, Khadrawy YA, El Sayed NS. Neuroprotective effect of PPAR alpha and gamma agonists in a mouse model of amyloidogenesis through modulation of the Wnt/beta catenin pathway via targeting alpha- and beta-secretases. *Prog Neuropsychopharmacol Biol Psychiatry* 2020, **97:** 109793.

Authors' contributions

G. Gao, X Yang, B Jiang, and P Jiang were involved in the concept and design of the study. W. Qi, Y. Long, Z. Li, Z. Zhao J. Shi, D Zhu, Z Zhao, W. Xie, L. Wang, T Zhou were responsible for conducting the experiments. W. Qi, Y. Long and T Zhou drafted the manuscript and G. Gao revised the manuscript. P Jiang, Y. Long and Z. Li were responsible for data analysis. All authors contributed to the interpretation of data

945 and provided revisions to the manuscript. G. Gao will act as guarantor for the study.
946 All authors read and approved the final manuscript. W. Qi, Y. Long and Z. Li
947 contributed equally to this study.
948
949 **Figure legend**
950 **Fig.1 Increased Kallistatin was presented in AD patients and could impair**
951 **cognitive memory in mice.** (A-B) Serum Kallistatin(A), fasting blood glucose
952 (FBG), triglyceride (TG), and total cholesterol (TC). (B) of AD patients and their
953 corresponding normal control subjects. (C-D) Serum Kallistatin(C), TG, and TC(D) of
954 AD patients with DM and their corresponding normal control subjects. The behavioral
955 performance of KAL-TG mice was assessed through the Morris water maze test. (E-
956 H), Y-maze test(I), and electrophysiology (J). (E)The escape latency time of different
957 months of KAL-TG mice (3M, 6M, 9M, 12M) and corresponding WT mice were
958 presented during 1-6 day. (F-H) Cognitive functions were evaluated by spatial probe
959 test at day 7, the representative each group mice traces were shown (F), then
960 analyzing each group mice crossing platform times (G) and time percent in the
961 targeted area (H), n=4 to 9 per group. (I) Spontaneous alternation of Y-maze test. (J)
962 LTP was measured by whole-cell voltage-clamp recordings of CA1 neurons in acute
963 hippocampal slices of KAL-TG (3M, 6M, 12M) and WT mice, n = 6-12 cells from 3
964 mice per group. Error bars represent the standard deviation (SD); one asterisk, $p <$
965 0.05, two asterisks, $p < 0.01$; three asterisks, $p < 0.001$; four asterisks, $p < 0.0001$.

966

967 **Fig.2 Kallistatin promoted Aβ generation.** (A-B) Immunohistochemistry staining of
968 Aβ(A) was carried out in KAL-TG and WT mice hippocampal tissue. *Scale bar*,
969 100μm. The statistical analysis of Aβ plaques (B) in hippocampal tissue of KAL-TG
970 and WT mice, n=4-5 per group. (C) Protein levels of Aβ were tested by western blot
971 analysis in hippocampal tissue, n=3 per group, then statistically analyzed the above
972 results. (D) Hippocampal tissue Aβ42 contents were performed by ELISA in KAL-TG
973 and WT groups, n=3 per group. (E) Primary mouse neurons were isolated, then
974 infected with adenovirus to overexpress Kallistatin for 72h. Aβ42 concentration of
975 primary hippocampal neurons supernate and cell lysate were quantified by ELISA,
976 n=3 per group. (F-G) Western blot analysis of Aβ protein level in primary
977 hippocampal neurons infected with overexpressing Kallistatin adenovirus and control
978 groups, then statistical analysis of Aβ protein levels, n=3 per group. Error bars
979 represent the standard deviation (SD); one asterisk, $p < 0.05$; two asterisks, $p < 0.01$;
980 three asterisks, $p < 0.001$.

981

982 **Fig.3 Kallistatin promoted tau phosphorylation.** (A-B) Immunohistochemistry
983 staining of phosphorylated tau (p-tau S396, p-tau T231, p-tau S202) and tau(A) was
984 carried out in KAL-TG and WT mice hippocampal tissue. Scale bar, 100μm. The
985 statistical analysis of phosphorylated tau(B) in hippocampal tissue of KAL-TG and
986 WT mice, n=3 per group. (C-D) Protein levels of phosphorylated tau (p-tau S396, p-

987 tau T231, p-tau S202) and tau were tested by western blot analysis in hippocampal
988 tissue, then statistically analyzed the above results. Error bars represent the standard
989 deviation (SD); one asterisk, $p < 0.05$; two asterisks, $p < 0.01$; three asterisks, $p <$
990 0.001.
991
992 **Fig.4 Kallistatin transgenic mice exhibited increased BACE1 expression and**
993 **activity in the hippocampus.** (A) Western blot analysis of relevant proteins, such as
994 APP, PS1, and BACE1 during Aβ generation in hippocampal tissue of each time point
995 (6M, 9M, 12M) KAL-TG mice and corresponding WT control groups, n=3 per group,
996 then statistical analysis of APP, PS1 and BACE1 protein levels. (B)
997 Immunohistochemistry staining of BACE1 was carried out in KAL-TG and WT mice
998 hippocampal tissue at each time point (6M, 9M, 12M). n=3 to 5 per group. *Scale bar*,
999 100 μm. (C) Statistical analysis of BACE1 immunohistochemistry staining, n=3 to 4
1000 per group. (D) ELISA measured the β-secretase activity of each group's hippocampal
1001 tissue, n=3 per group. Error bars represent the standard deviation (SD); one asterisk, p
1002 < 0.05, two asterisks, $p < 0.01$.
1003
1004 **Fig.5 *In vitro*, Kallistatin promoted BACE1 expression to augment Aβ by**
1005 **suppressing PPARγ activation.** (A) The relevant protein levels in primary mouse
1006 neurons infected with overexpressing Kallistatin adenovirus during Aβ generation
1007 were determined by western blot analysis. (B) Statistical analysis of BACE1

1008 expression in primary neurons. (C-D) β-secretase (C) and γ- secretase (D) activity of
1009 primary hippocampal neurons infected with overexpressing Kallistatin adenovirus and
1010 control adenovirus was measured by ELISA. (E) Primary hippocampal neurons were
1011 treated with BACE1 inhibitor verubecestat (50nM), then infected with adenovirus to
1012 overexpress Kallistatin. Western blot analysis of Aβ, BACE1, and Kallistatin protein
1013 levels, β-actin served as a loading control. (F) HT22 cells were infected with BACE1
1014 siRNA, then infected with adenovirus to overexpress Kallistatin. Western blot
1015 analysis of Aβ and BACE1 protein levels, β-actin served as a loading control. (G) The
1016 relevant proteins involved in BACE1 transcriptional expressions, such as PPARγ,
1017 YY1, and SP1 were measured by western blot analysis in hippocampal tissue. β-actin
1018 served as a loading control. (H) Statistical analysis of PPARγ in hippocampal tissue of
1019 each group. (I) The representative diagrams of PPARγ expression in hippocampal
1020 tissue were presented in the above graphs. *Scale bar*, 100μm. (J) Statistical analysis of
1021 PPARγ immunohistochemistry staining in hippocampal tissue of each group, n=3 to 4
1022 per group. (K)Primary hippocampal neurons were treated with PPARγ agonist
1023 rosiglitazone (10nM) for 12h, then infected with adenovirus to overexpress Kallistatin
1024 for 72h. Western blot analysis of Aβ and BACE1 protein levels. β-actin served as a
1025 loading control. (L) Statistical analysis of PPARγ protein levels in each group. Error
1026 bars represent the standard deviation (SD), one asterisk, $p < 0.05$, two asterisks, $p <$
1027 0.01; three asterisks, $p < 0.001$; ns means no significant difference.
1028

1029 **Fig.6 Kallistatin directly bonded to the Notch1 receptor, which activated the**
1030 **Notch1 pathway to promote Aβ production.** (A) Notch1 expression was measured
1031 by western blot analysis in hippocampal tissue. β-actin served as a loading control.
1032 (B) Statistical analysis of Notch1 in hippocampal tissue of each group. (C) The
1033 representative diagrams of Nocth1 expression in hippocampal tissue were presented in
1034 the above graphs. Scale bar, 100μm. (D) Statistical analysis of Notch1
1035 immunohistochemistry staining in hippocampal tissue of each group. (E-F) Primary
1036 hippocampal neurons were infected with overexpressing Kallistatin adenovirus for
1037 72h, then Co-IP analysis (E) and membrane extraction experiment (F) was performed
1038 to verify whether Kallistatin can bind to the Notch1 receptor. β-actin served as a
1039 loading control. (G-H) HT22 cells were treated with siRNA (Notch1) and shRNA
1040 (HES1) to knock down Notch1 and HES1 for 12h, then infected with adenovirus to
1041 overexpress Kallistatin for 24h. Western blot analysis was used to detect the Notch1
1042 signaling pathway. Error bars represent the standard deviation (SD), one asterisk, $p <$
1043 0.05.
1044
1045 **Fig.7 Kallistatin promoted phosphorylation of tau by suppressing Wnt signaling**
1046 **pathway.** (A-B) GSK-3β and p-GSK-3β expression was measured by western blot
1047 analysis in hippocampal tissue, then statistically analyzed the above results. (C-D)
1048 Primary hippocampal neurons were treated with overexpressing Kallistatin adenovirus
1049 for 72h, then western blot analysis was used to detect the content of GSK-3β, p-GSK-

1050 3β, tau, p-tau (Ser9, T231, S396), and statistically analyzed the above results. (E-F)
1051 Primary hippocampal neurons were treated with overexpressing Kallistatin adenovirus
1052 for 48h, then treated with LiCl (10mM) for 24h, western blot analysis was used to
1053 detect the content of GSK-3β, p-GSK-3β, p-tau (Ser9, T231, S396), and statistical
1054 analysis of the above results.
1055
1056 **Fig.8 Fenofibrate could alleviate memory and cognitive impairment of KAL-TG**
1057 **mice.** (A) Illustration of experimental protocols. Fenofibrate (0.3 g/kg/d × 5week, i.g.)
1058 or rosiglitazone (5mg/kg/d × 5week, i.g.) were given to KAL-TG mice. The serum for
1059 Kallistatin measuring was collected at week 0 and week 4. And Morris water maze
1060 and Y-maze test were performed at week 5. (B-E) Behavioral performance was
1061 assessed through the Morris water maze test (B-E) and the Y-maze test (F). (B) The
1062 escape latency time was presented during 1-5 day. (C-E) Cognitive functions were
1063 evaluated by spatial probe test at day 6, then analyzing each group of mice crossing
1064 platform times(C), time percent in the targeted area (D), and the path traces heatmap
1065 (E), n=5 to 6 per group. (F) Spontaneous alternation of Y-maze test. (G) Kallistatin
1066 decreased ratio was calculated by dividing the serum Kallistatin concentration of
1067 KAL-TG mice before Fenofibrate/ rosiglitazone treatment by the serum Kallistatin
1068 concentration of KAL-TG mice after a-month treatment, and serum Kallistatin
1069 concentration was measured by ELISA. (H) Protein levels of Aβ, BACE1, p-tau, tau,
1070 p-GSK-3β and GSK-3β were tested by western blot analysis in hippocampal tissue.

1071 Error bars represent the standard deviation (SD); one asterisk, $p < 0.05$.

1072

Table.S1 Clinical characteristic of AD patients

	NC	AD	*p value* *(Dementia vs NC)*
N	61	56	NA
Age	49-82	52-85	****
Average age	64±8.53	73.02±9.43	NA
Male	29	25	NS
Female	32	31	
GLU (mmol/L)	5.07±0.65	6.73±2.81	****
TC (mmol/L)	4.63±0.58	4.50±1.12	NS
TG (mmol/L)	1.09±0.50	1.41±0.65	**

N is an abbreviation for number; GLU is an abbreviation for glucose; TC is an abbreviation for total cholesterol; TG is an abbreviation for triglyceride; NA indicates not available; NS indicates no significance. two asterisk, $p < 0.01$, four asterisk, $p < 0.0001$.

Table.S2 Clinical characteristic of AD patients with DM

	NC	AD + DM	*p value* *(Dementia+DM vs NC)*
N	61	26	NA
Age	49-82	52-92	****
Average age	64±8.53	76.77±8.69	NA
Male	29	15	NS
Female	32	11	
GLU (mmol/L)	5.07±0.65	8.12±3.05	****
TC (mmol/L)	4.63±0.58	4.29±1.04	NS
TG (mmol/L)	1.08±0.50	1.69±0.68	****

1080 N is an abbreviation for number; GLU is an abbreviation for glucose; TC is an
1081 abbreviation for total cholesterol; TG is an abbreviation for triglyceride; NA indicates
1082 not available; NS indicates no significance. four asterisk, $p < 0.0001$.
1083
1084 Figure legend
1085 Fig.S1 (A-B) GAD disease enrichment analysis (A) and PFAM analysis (B) result.
1086 Differentially expressed genes in neurons were obtained from GSE161355, and GAD
1087 disease enrichment was analyzed on David database. (C-D) Western blot analysis of
1088 Kallistatin expression in aging model SAMP8 and corresponding control SAMR1
1089 mice hippocampal tissue samples, then statistically analyzing the above results. β-
1090 Actin served as a loading control. Error bars represent the standard deviation (SD);
1091 three asterisks, $p < 0.001$.
1092
1093 Fig.S2 (A) HT22 cells were infected with adenovirus to overexpress Kallistatin for
1094 48h. Aβ42 concentration of supernate and cell lysate was quantified by ELISA. (B-C)
1095 Western blot analysis of Aβ protein level in HT22 cells infected with overexpressing
1096 Kallistatin adenovirus and control groups for 48h, then statistical analysis of
1097 Kallstatin protein levels. (D) BACE1 mRNA expression in hippocampal tissue. (E) α-
1098 secretases (ADAM9, ADAM10, ADAM17) mRNA expression in hippocampal tissue.
1099 (F) γ-secretase activity of each group's hippocampal tissue was measured by ELISA.
1100 (G) Primary hippocampal neurons were identified with MAP2. Error bars represent

1101 the standard deviation (SD), one asterisk, $p < 0.05$, two asterisks, $p < 0.01$.

1102

1103 Fig.S3 (A) The relevant protein levels in HT22 cells infected with overexpressing
1104 Kallistatin adenovirus during Aβ generation were determined by western blot
1105 analysis. (B) Statistical analysis of BACE1 expression in HT22 cells. (C) β-secretase
1106 activity of HT22 cells infected with overexpressing Kallistatin adenovirus and control
1107 adenovirus was measured by ELISA. (D) Primary hippocampal neurons were infected
1108 with BACE1 siRNA for 72h. Western blot analysis of BACE1 protein levels. (E)
1109 HT22 cells were treated with PPARγ agonist rosiglitazone (10nM) for 12h, then
1110 infected with adenovirus to overexpress Kallistatin for 48h. Western blot analysis of
1111 Aβ and BACE1 protein levels. β-actin served as a loading control. Error bars
1112 represent the standard deviation (SD), two asterisks, $p < 0.01$.

1113

1114 Fig.S4 (A-B) Western blot analysis of Notch1 protein level in primary hippocampal
1115 neurons and HT22 cells infected with overexpressing Kallistatin adenovirus and
1116 control groups. (C) HT22 cells were infected with overexpressing Kallistatin
1117 adenovirus for 48h, and Co-IP analysis was conducted to verify whether Kallistatin
1118 can bind to the Notch1 receptor. β-actin served as a loading control. (D) Primary
1119 hippocampal neurons were treated with Kallistatin protein for 72h, then IP analysis.
1120 (E) Primary hippocampal neurons were infected with Notch1 siRNA for 72h. Western
1121 blot analysis of BACE1 protein levels. (F) HT22 cells were infected with HES1

1122 shRNA for 48h. Western blot analysis of HES1 protein levels.

1123

1124 Fig.S5 (A) Western blot analysis of GSK-3β, p-GSK-3β, tau, p-tau(Ser9, T231, S396)

1125 in HT22 cells infected with overexpressing Kallistatin adenovirus and control groups.

1126 (B) Western blot analysis of GSK-3β, p-GSK-3β, p-tau(Ser9, T231, S396) in HT22

1127 cells infected with overexpressing Kallistatin adenovirus and control groups for 24h,

1128 then treated with LiCl(10 mM) for 24h.

1129

Fig.1

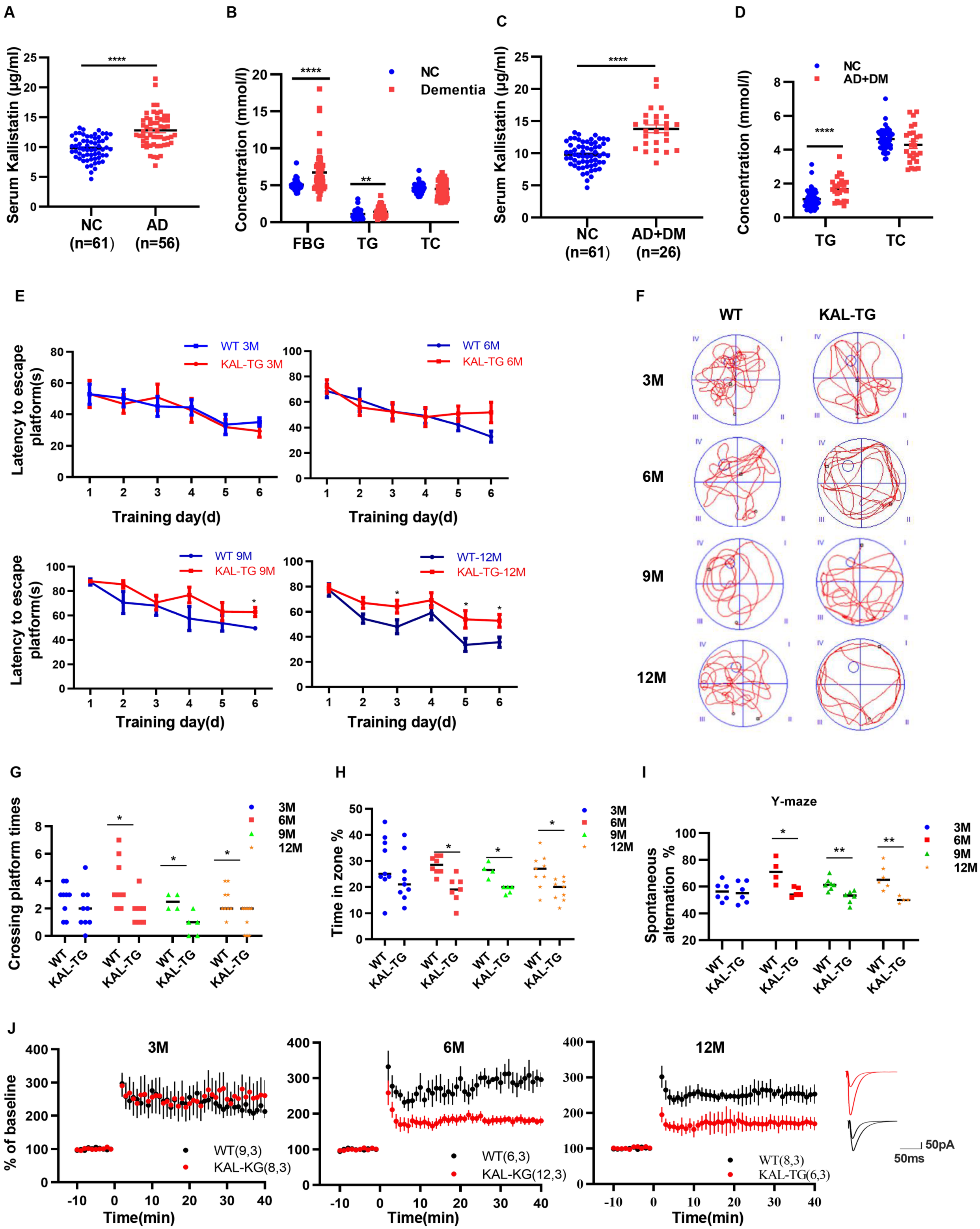
A
Serum Kallistatin (μg/ml)
****
NC (n=61)
AD (n=56)
B
Concentration (mmol/l)
****
**
NC
Dementia
FBG
TG
TC
C
Serum Kallistatin (μg/ml)
****
NC (n=61)
AD+DM (n=26)
D
Concentration (mmol/l)
NC
AD+DM
****
TG
TC
E
Latency to escape platform(s)
WT 3M
KAL-TG 3M
WT 6M
KAL-TG 6M
WT 9M
KAL-TG 9M
WT-12M
KAL-TG-12M
Training day(d)
F
WT
KAL-TG
3M
6M
9M
12M
G
Crossing platform times
3M
6M
9M
12M
WT
KAL-TG
H
Time in zone %
I
Y-maze
Spontaneous alternation %
J
3M
6M
12M
% of baseline
WT(9,3)
KAL-KG(8,3)
WT(6,3)
KAL-KG(12,3)
WT(8,3)
KAL-TG(6,3)
Time(min)
50pA
50ms

Fig.2

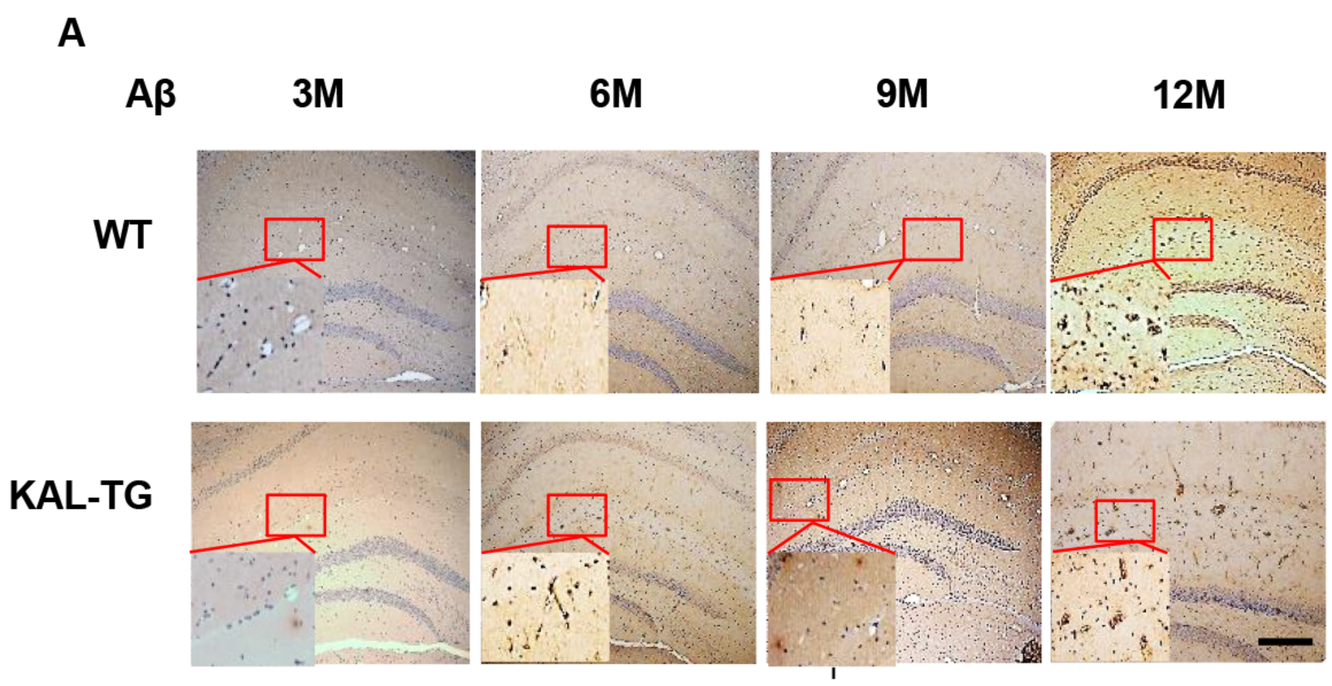
A
Aβ
3M
6M
9M
12M
WT
KAL-TG

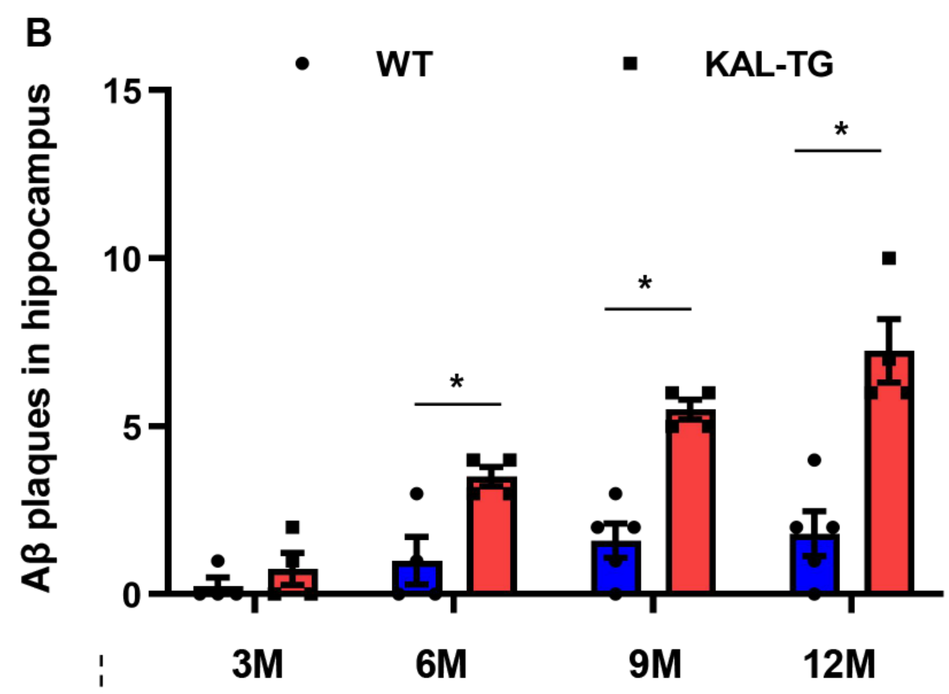
B
WT
KAL-TG
Aβ plaques in hippocampus
15
10
5
0
*
*
*
3M
6M
9M
12M

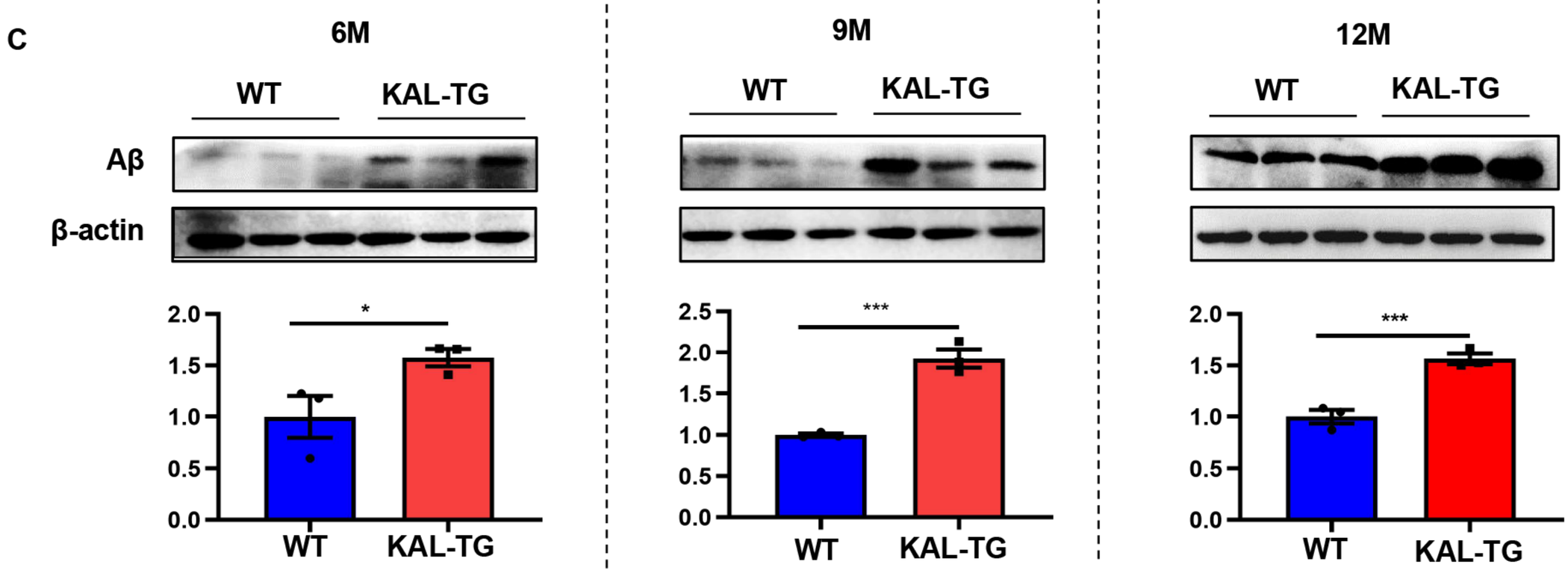
C
6M
9M
12M
WT
KAL-TG
Aβ
β-actin
2.0
1.5
1.0
0.5
0.0
*
***
***
WT
KAL-TG

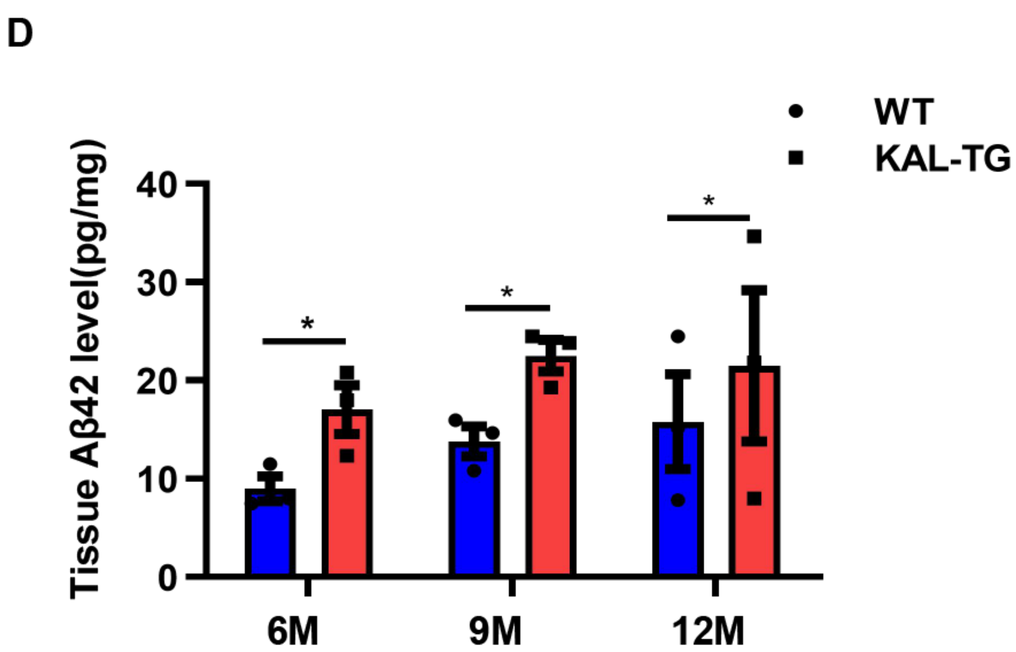
D
WT
KAL-TG
Tissue Aβ42 level(pg/mg)
40
30
20
10
0
*
*
*
6M
9M
12M

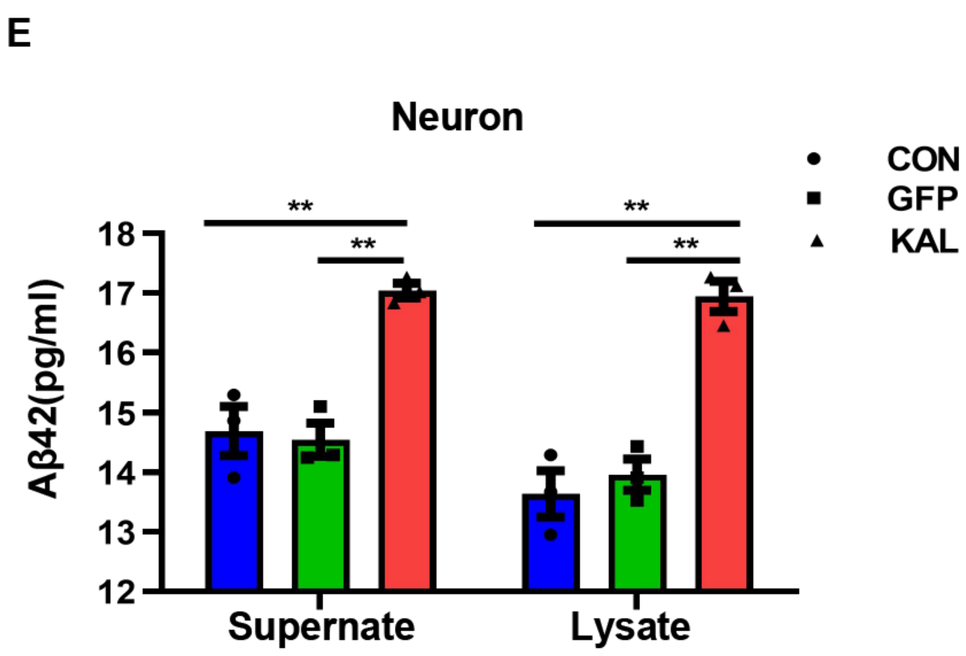
E
Neuron
CON
GFP
KAL
Aβ42(pg/ml)
18
17
16
15
14
13
12
**
**
**
**
Supernate
Lysate

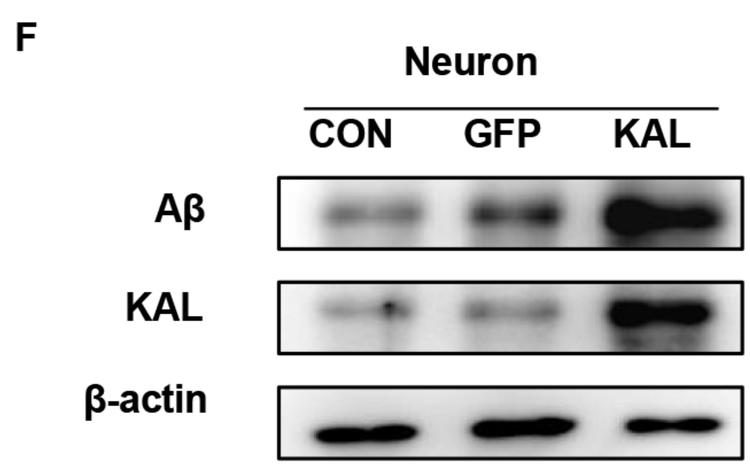
F
Neuron
CON
GFP
KAL
Aβ
KAL
β-actin

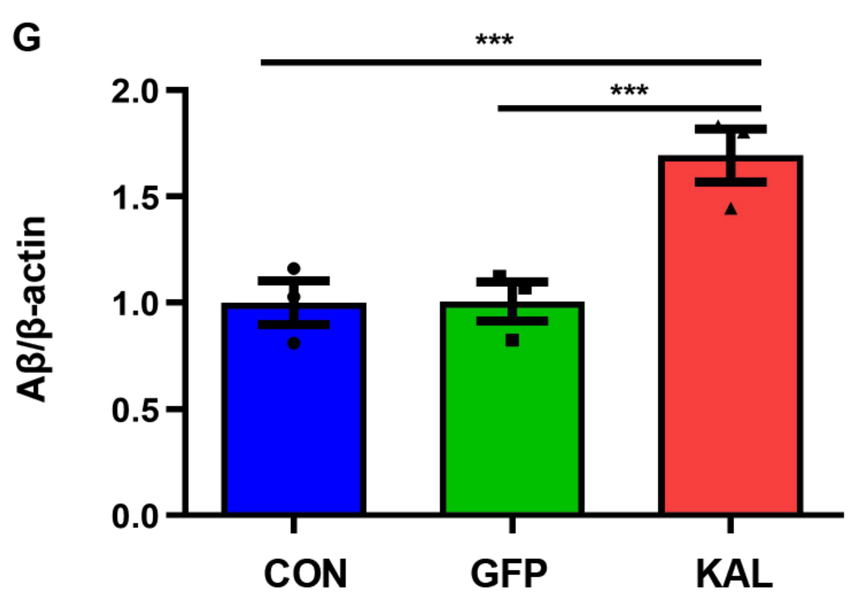
G
***
***
Aβ/β-actin
2.0
1.5
1.0
0.5
0.0
CON
GFP
KAL

Fig.3

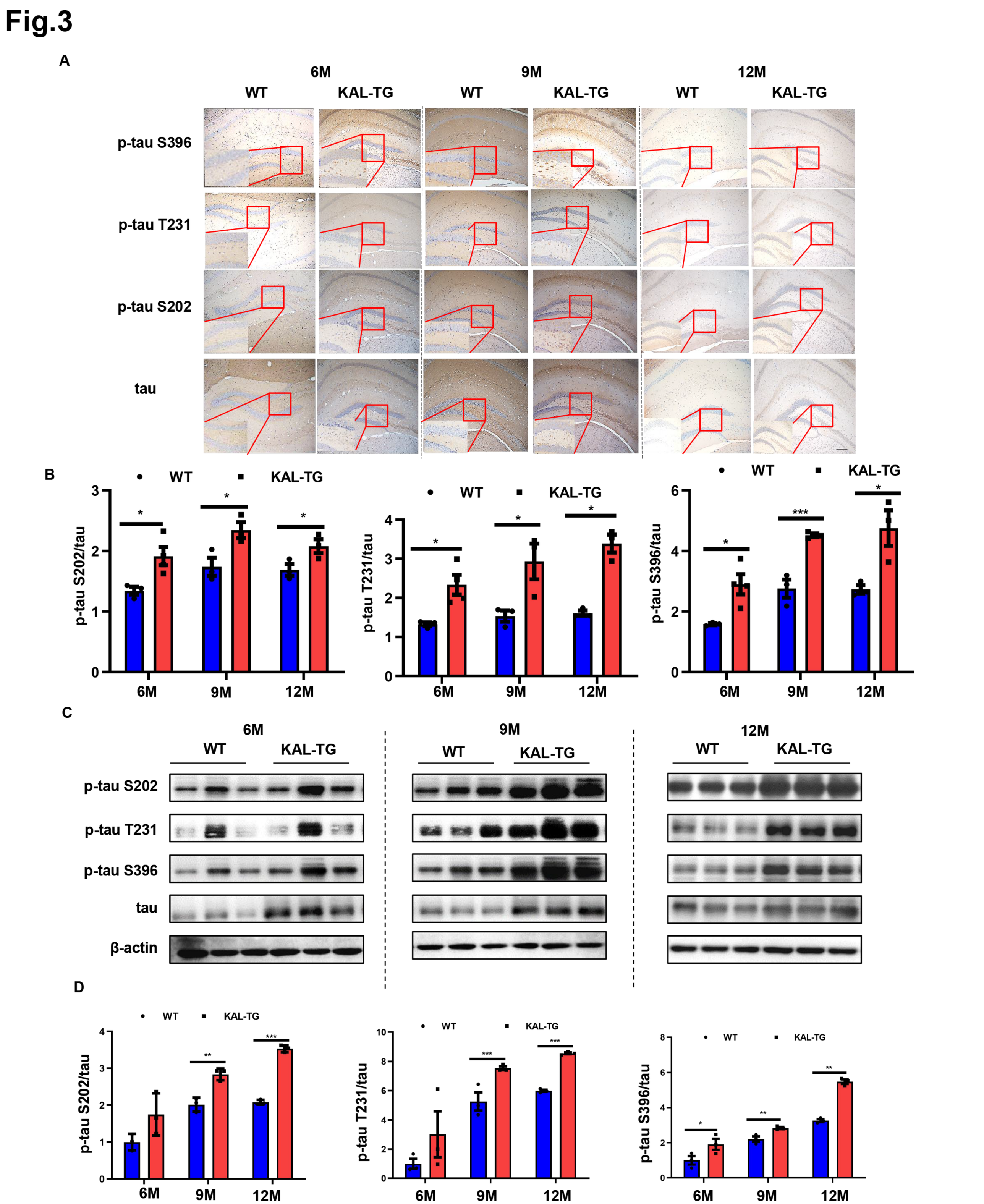
A
6M
9M
12M
WT
KAL-TG
p-tau S396
p-tau T231
p-tau S202
tau
B
WT
KAL-TG
p-tau S202/tau
p-tau T231/tau
p-tau S396/tau
6M
9M
12M
C
β-actin
D

Fig.4

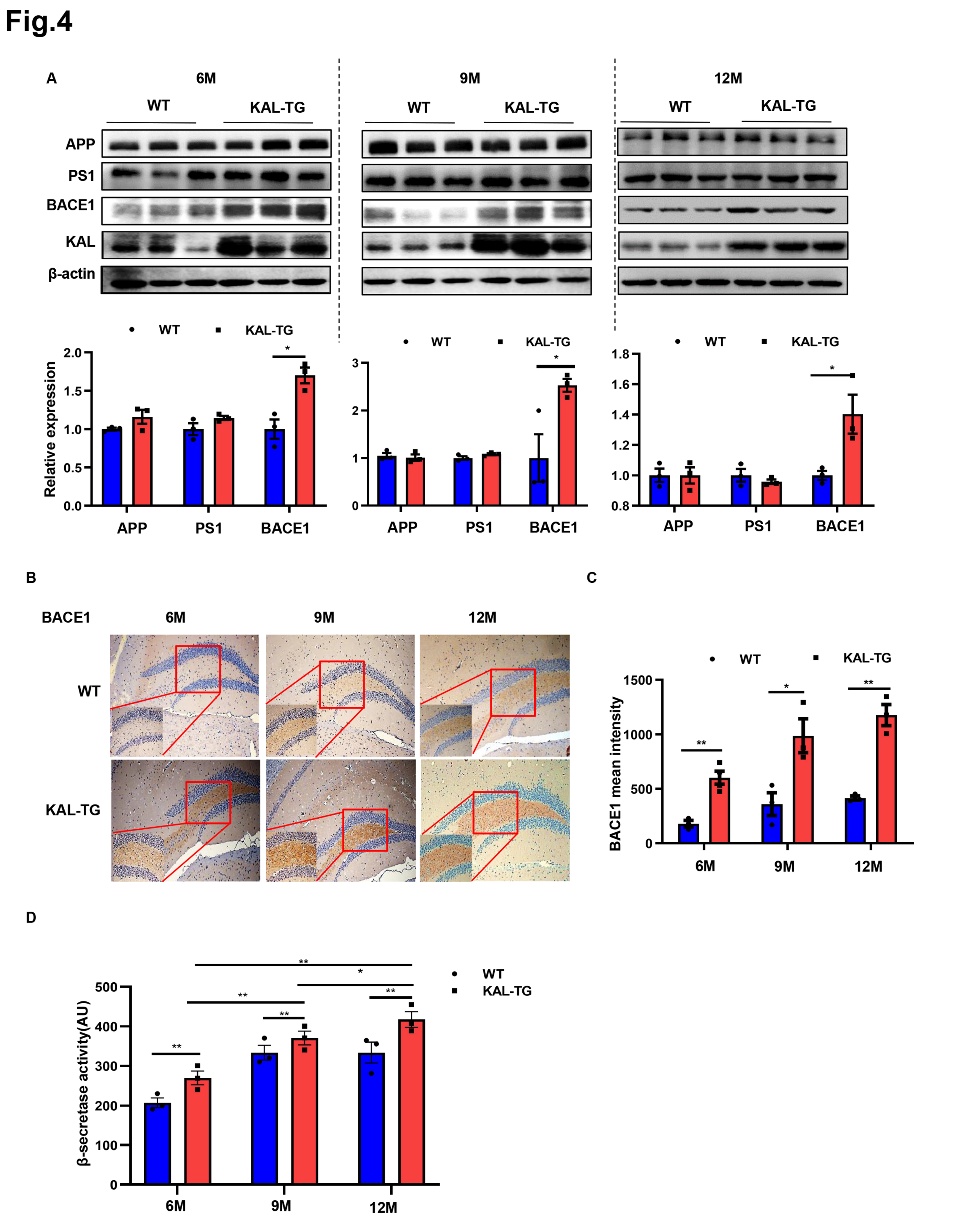
A
6M
9M
12M
WT
KAL-TG
APP
PS1
BACE1
KAL
β-actin
Relative expression
B
BACE1
C
BACE1 mean intensity
D
β-secretase activity(AU)

Fig.5

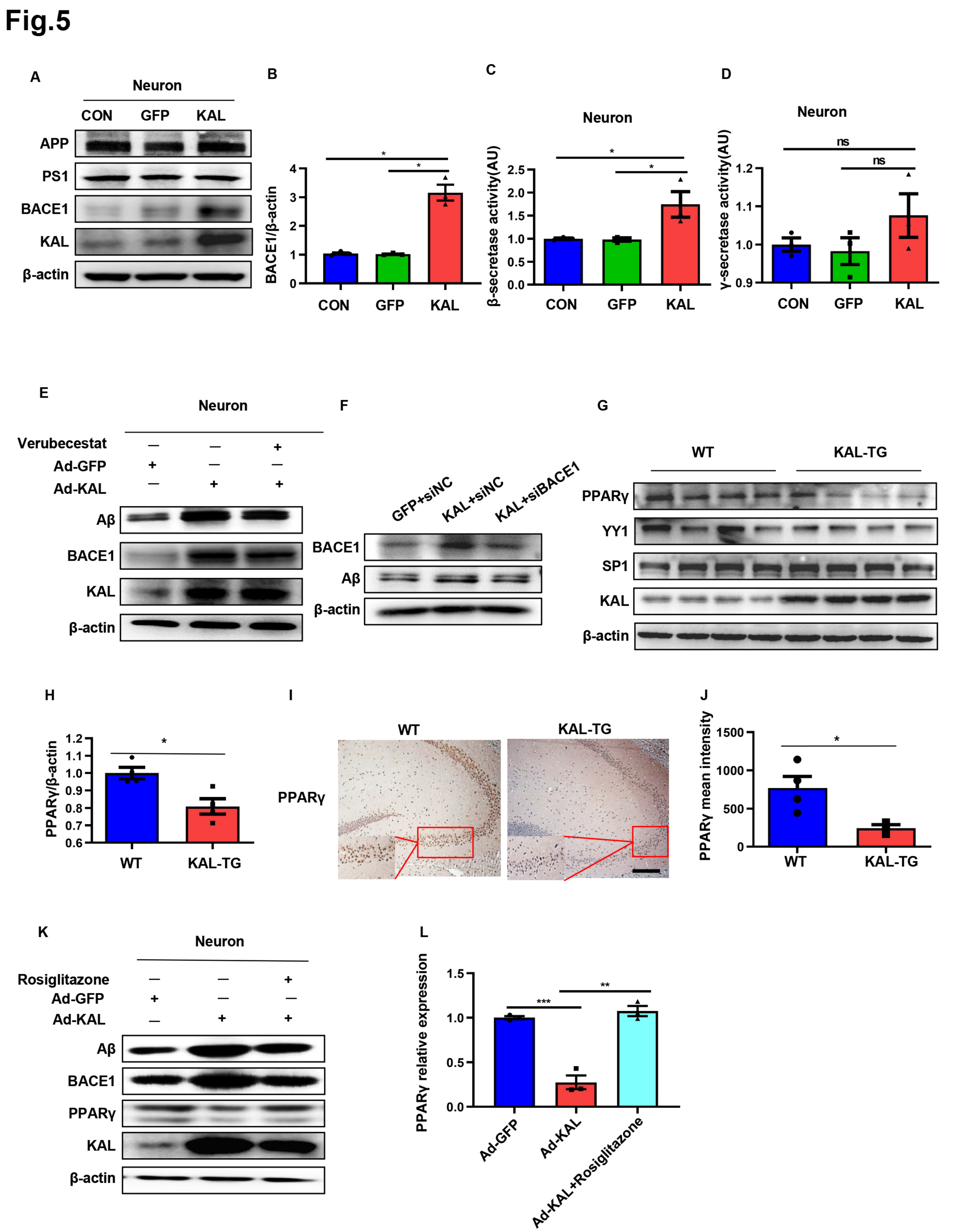
A
Neuron
CON
GFP
KAL
APP
PS1
BACE1
KAL
β-actin
B
BACE1/β-actin
CON
GFP
KAL
C
Neuron
β-secretase activity(AU)
CON
GFP
KAL
D
Neuron
γ-secretase activity(AU)
ns
ns
CON
GFP
KAL
E
Neuron
Verubecestat
Ad-GFP
Ad-KAL
Aβ
BACE1
KAL
β-actin
F
GFP+siNC
KAL+siNC
KAL+siBACE1
BACE1
Aβ
β-actin
G
WT
KAL-TG
PPARγ
YY1
SP1
KAL
β-actin
H
PPARγ/β-actin
WT
KAL-TG
I
WT
KAL-TG
PPARγ
J
PPARγ mean intensity
WT
KAL-TG
K
Neuron
Rosiglitazone
Ad-GFP
Ad-KAL
Aβ
BACE1
PPARγ
KAL
β-actin
L
PPARγ relative expression
Ad-GFP
Ad-KAL
Ad-KAL+Rosiglitazone

Fig.6

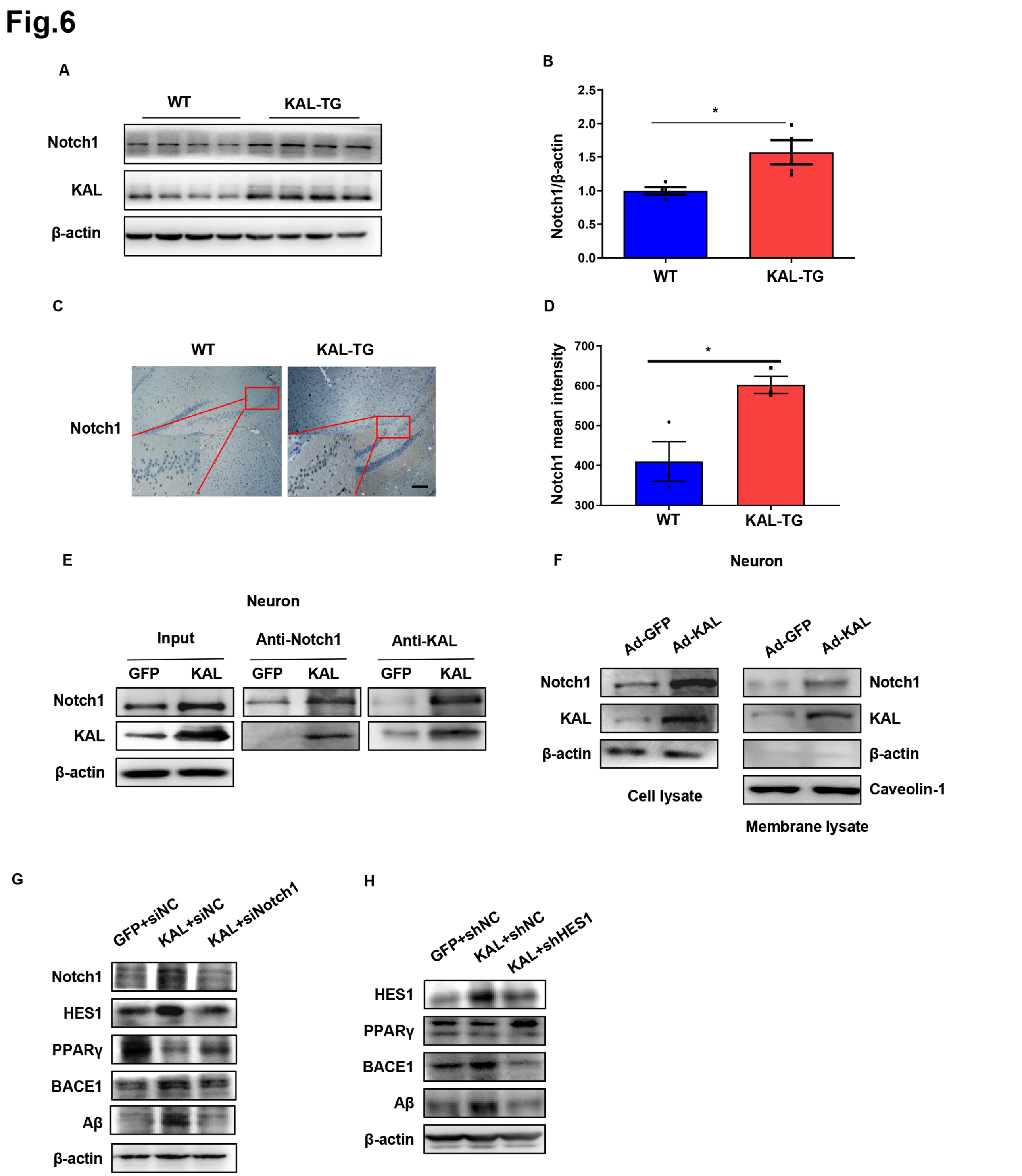
A
WT
KAL-TG
Notch1
KAL
β-actin
B
Notch1/β-actin
2.5
2.0
1.5
1.0
0.5
0.0
*
WT
KAL-TG
C
WT
KAL-TG
Notch1
D
Notch1 mean intensity
700
600
500
400
300
*
WT
KAL-TG
E
Neuron
Input
Anti-Notch1
Anti-KAL
GFP
KAL
GFP
KAL
GFP
KAL
Notch1
KAL
β-actin
F
Neuron
Ad-GFP
Ad-KAL
Ad-GFP
Ad-KAL
Notch1
KAL
β-actin
Cell lysate
Notch1
KAL
β-actin
Caveolin-1
Membrane lysate
G
GFP+siNC
KAL+siNC
KAL+siNotch1
Notch1
HES1
PPARγ
BACE1
Aβ
β-actin
H
GFP+shNC
KAL+shNC
KAL+shHES1
HES1
PPARγ
BACE1
Aβ
β-actin

Fig.7

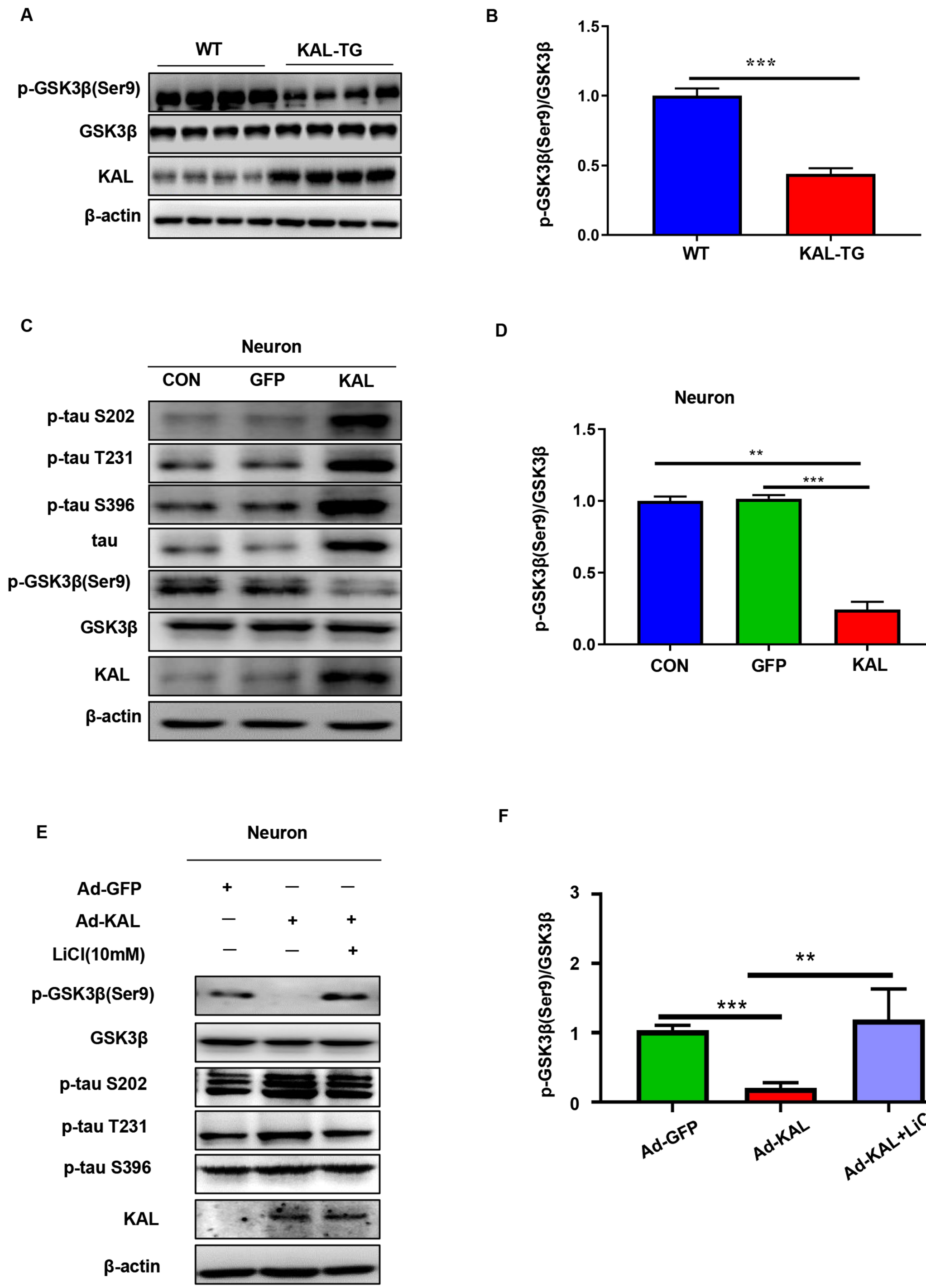
A
WT
KAL-TG
p-GSK3β(Ser9)
GSK3β
KAL
β-actin
B
p-GSK3β(Ser9)/GSK3β
1.5
1.0
0.5
0.0
***
WT
KAL-TG
C
Neuron
CON
GFP
KAL
p-tau S202
p-tau T231
p-tau S396
tau
p-GSK3β(Ser9)
GSK3β
KAL
β-actin
D
Neuron
p-GSK3β(Ser9)/GSK3β
1.5
1.0
0.5
0.0
**
***
CON
GFP
KAL
E
Neuron
Ad-GFP
Ad-KAL
LiCl(10mM)
p-GSK3β(Ser9)
GSK3β
p-tau S202
p-tau T231
p-tau S396
KAL
β-actin
F
p-GSK3β(Ser9)/GSK3β
3
2
1
0
**
***
Ad-GFP
Ad-KAL
Ad-KAL+LiCl

Fig.8

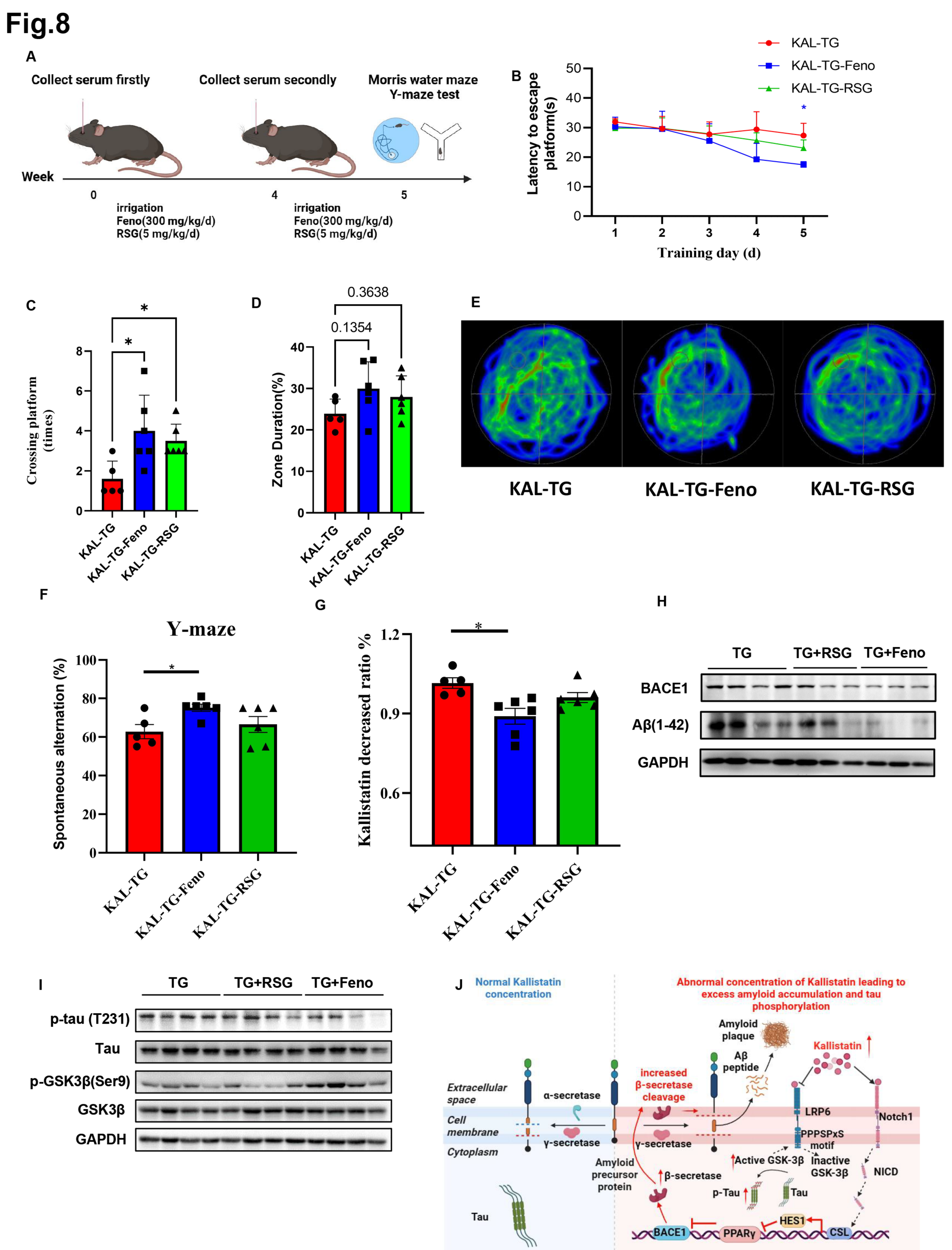
A
Collect serum firstly
Collect serum secondly
Morris water maze
Y-maze test
Week
0
4
5
irrigation
Feno(300 mg/kg/d)
RSG(5 mg/kg/d)
irrigation
Feno(300 mg/kg/d)
RSG(5 mg/kg/d)
B
KAL-TG
KAL-TG-Feno
KAL-TG-RSG
Latency to escape platform(s)
Training day (d)
C
Crossing platform (times)
KAL-TG
KAL-TG-Feno
KAL-TG-RSG
D
0.3638
0.1354
Zone Duration(%)
E
KAL-TG
KAL-TG-Feno
KAL-TG-RSG
F
Y-maze
Spontaneous alternation (%)
G
Kallistatin decreased ratio %
H
TG
TG+RSG
TG+Feno
BACE1
Aβ(1-42)
GAPDH
I
TG
TG+RSG
TG+Feno
p-tau (T231)
Tau
p-GSK3β(Ser9)
GSK3β
GAPDH
J
Normal Kallistatin concentration
Abnormal concentration of Kallistatin leading to excess amyloid accumulation and tau phosphorylation
Extracellular space
Cell membrane
Cytoplasm
α-secretase
γ-secretase
Amyloid precursor protein
increased β-secretase cleavage
Amyloid plaque
Aβ peptide
Kallistatin
LRP6
Notch1
PPPSPxS motif
Active GSK-3β
Inactive GSK-3β
NICD
β-secretase
p-Tau
Tau
HES1
BACE1
PPARγ
CSL

Fig.S1

A

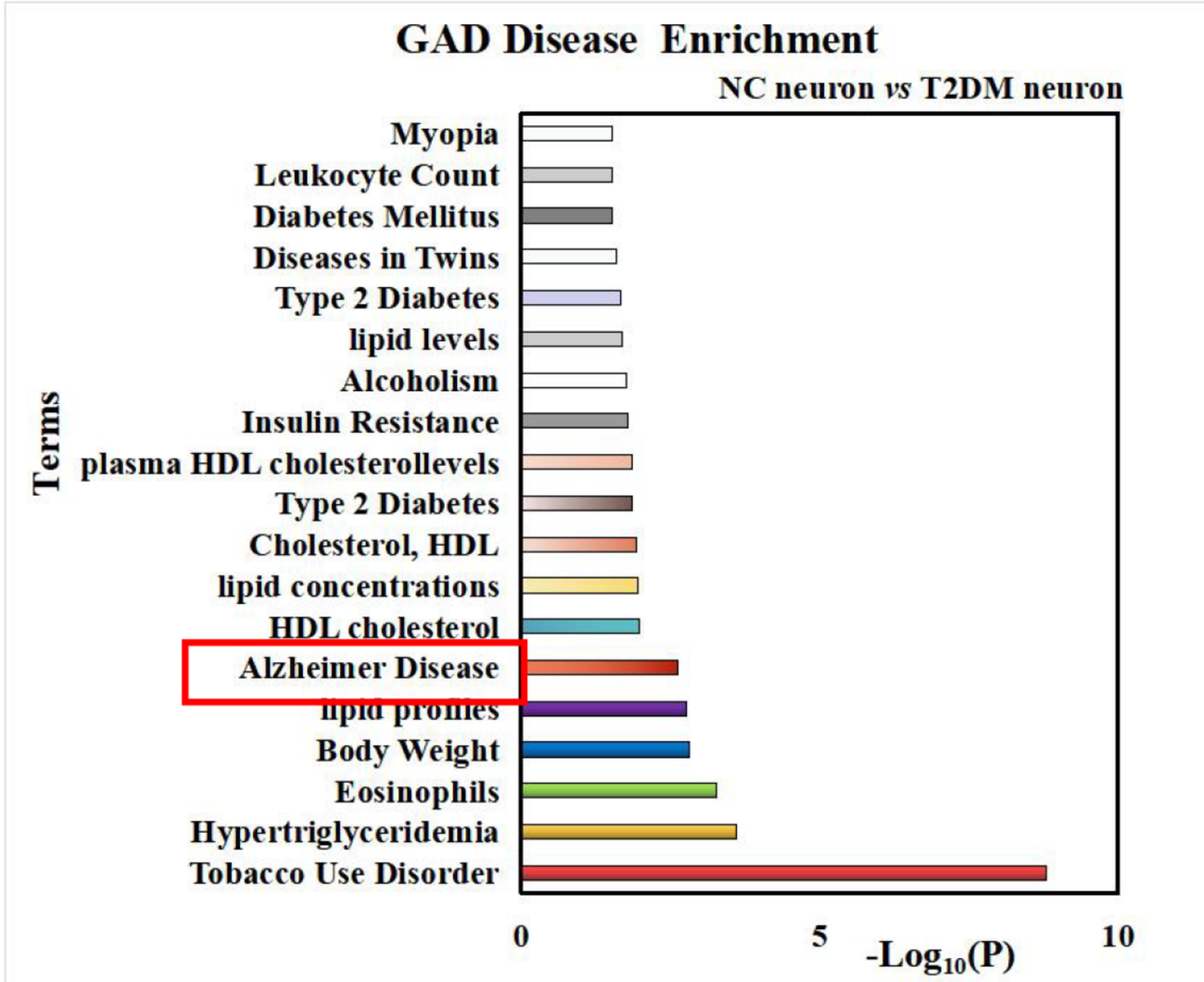
GAD Disease Enrichment
NC neuron vs T2DM neuron
Terms
Myopia
Leukocyte Count
Diabetes Mellitus
Diseases in Twins
Type 2 Diabetes
lipid levels
Alcoholism
Insulin Resistance
plasma HDL cholesterollevels
Type 2 Diabetes
Cholesterol, HDL
lipid concentrations
HDL cholesterol
Alzheimer Disease
lipid profiles
Body Weight
Eosinophils
Hypertriglyceridemia
Tobacco Use Disorder
0
5
10
-Log10(P)

B

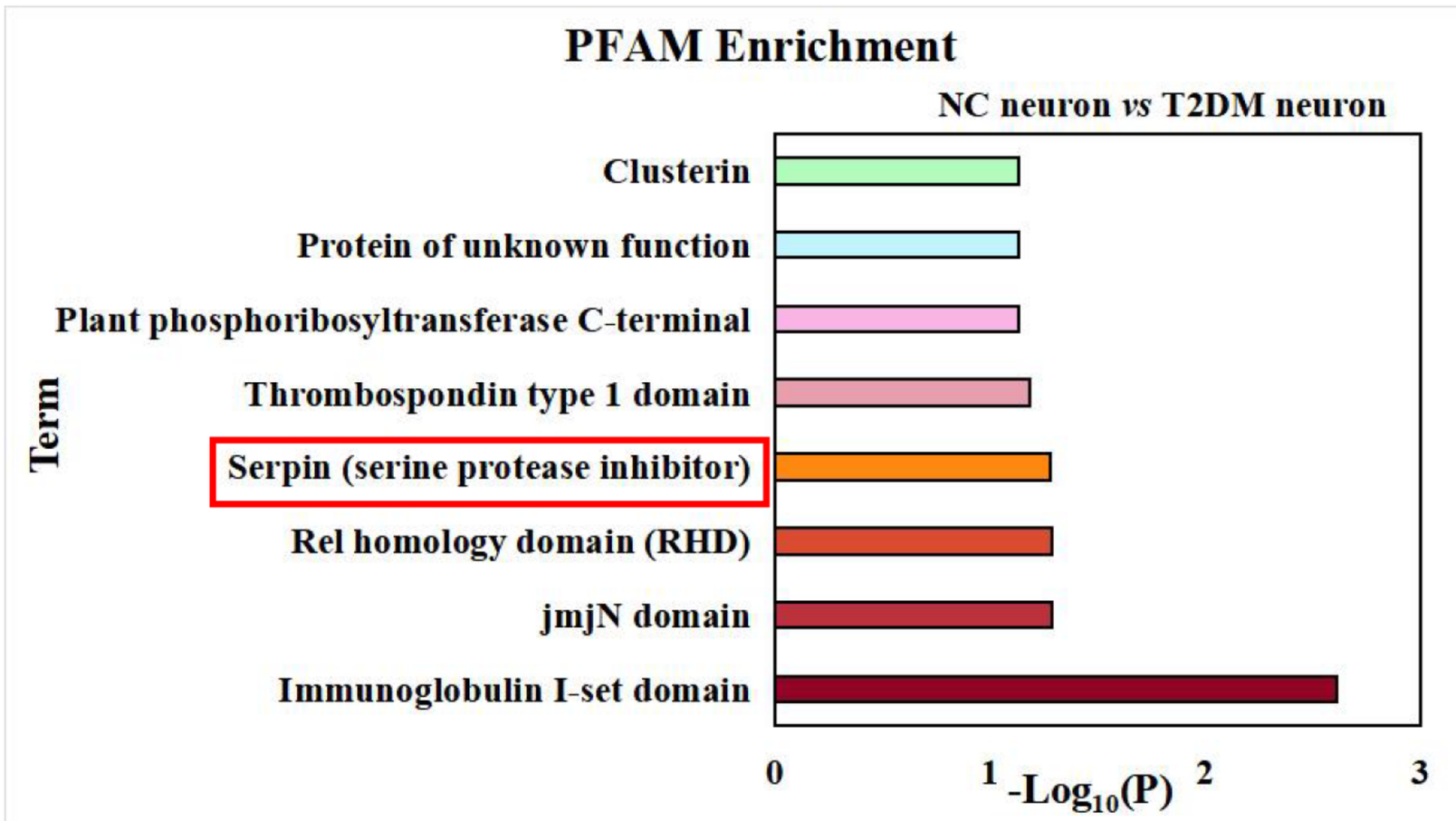
PFAM Enrichment
NC neuron vs T2DM neuron
Term
Clusterin
Protein of unknown function
Plant phosphoribosyltransferase C-terminal
Thrombospondin type 1 domain
Serpin (serine protease inhibitor)
Rel homology domain (RHD)
jmjN domain
Immunoglobulin I-set domain
0
1
2
3
-Log10(P)

C

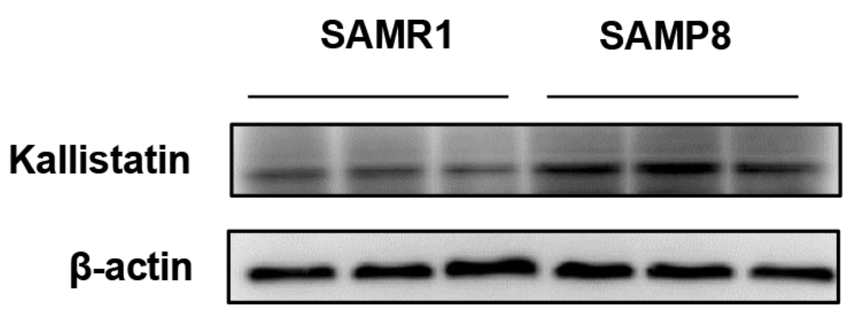
SAMR1
SAMP8
Kallistatin
β-actin

D

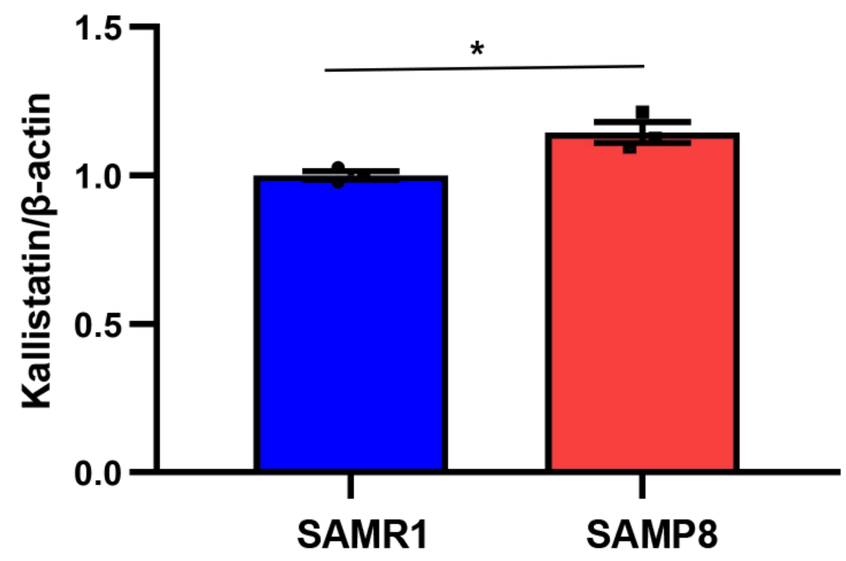
1.5
1.0
0.5
0.0
Kallistatin/β-actin
*
SAMR1
SAMP8

Fig.S2

A

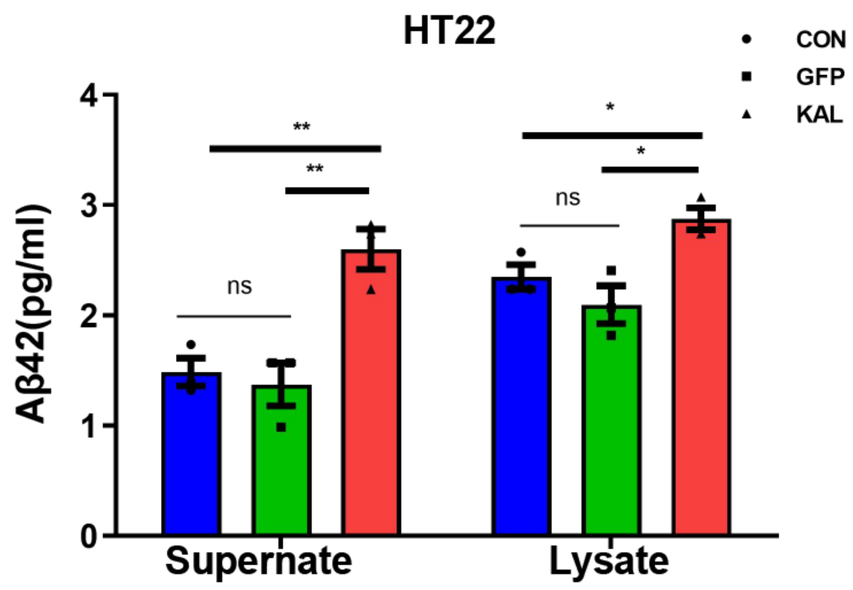

B

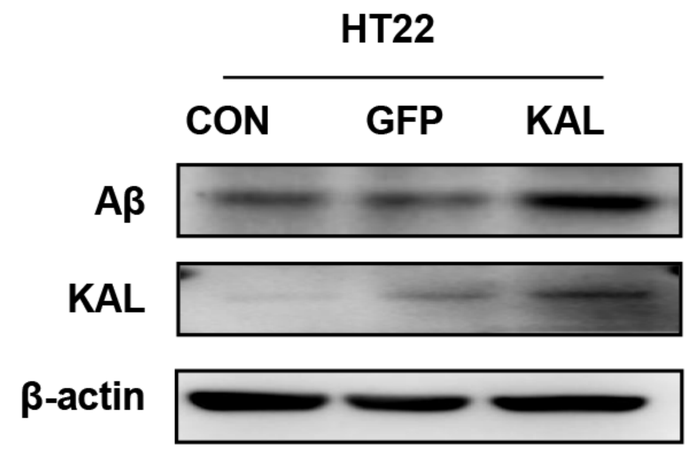

C

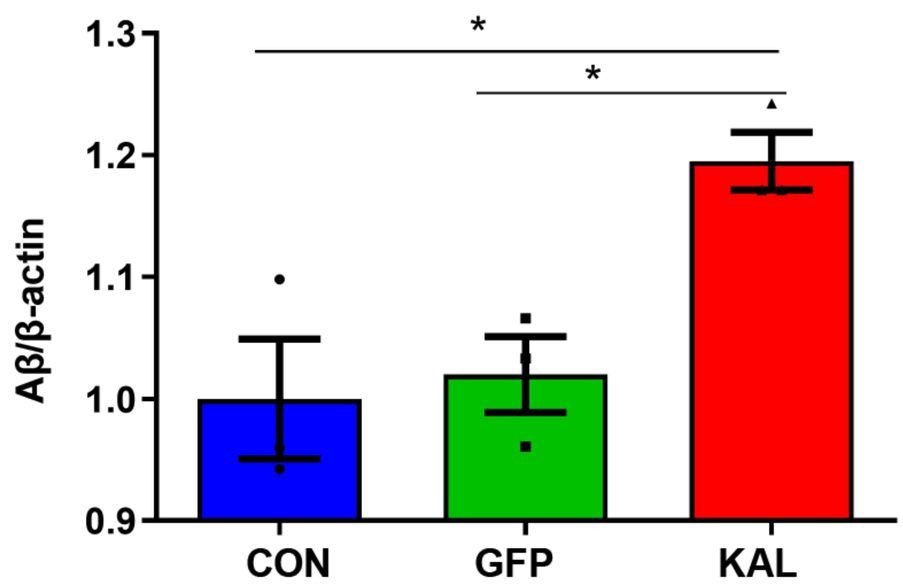

D

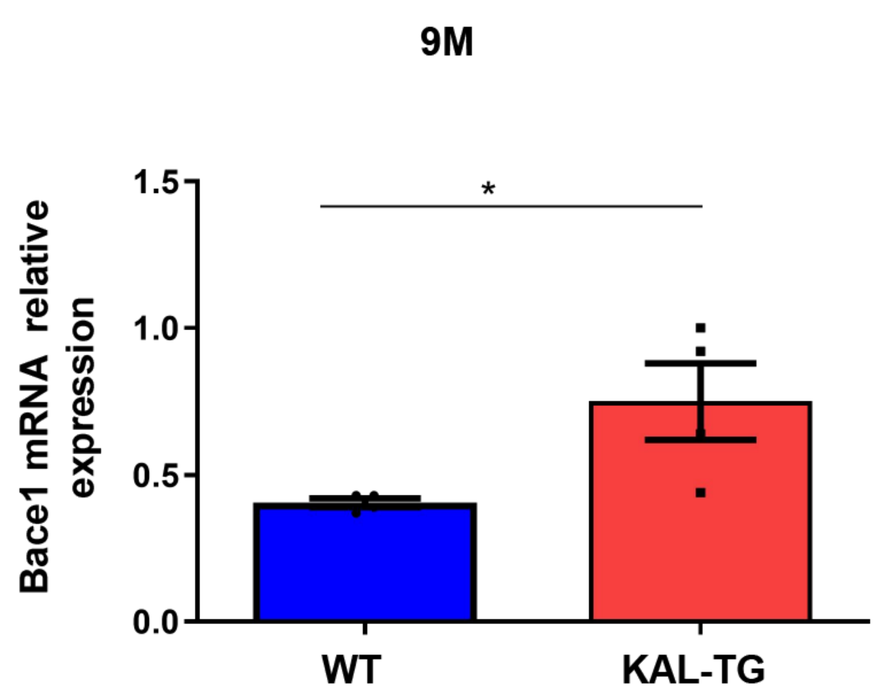

E

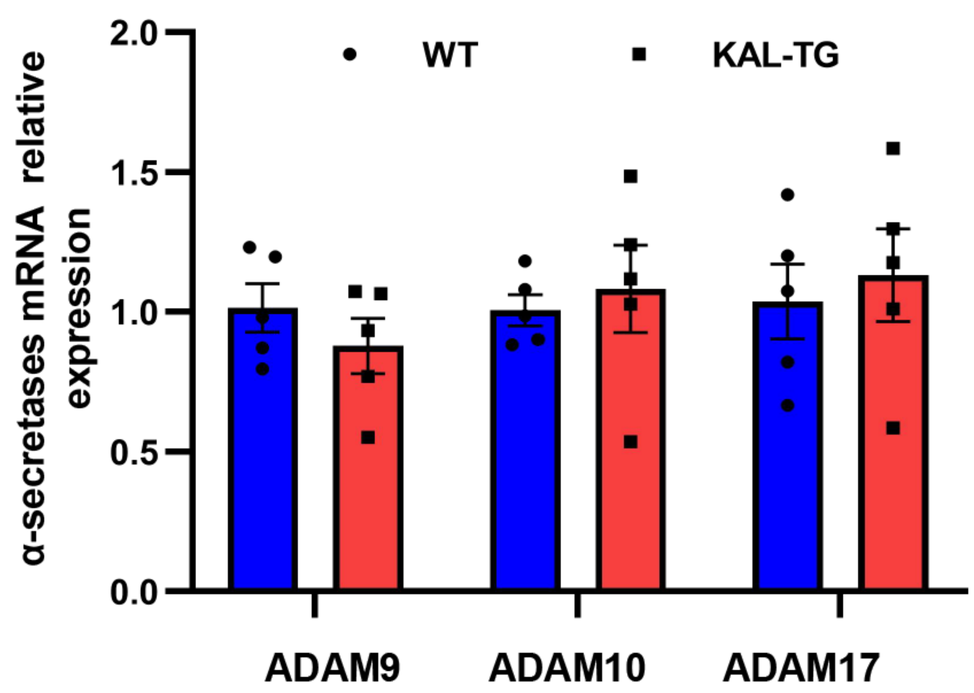

F

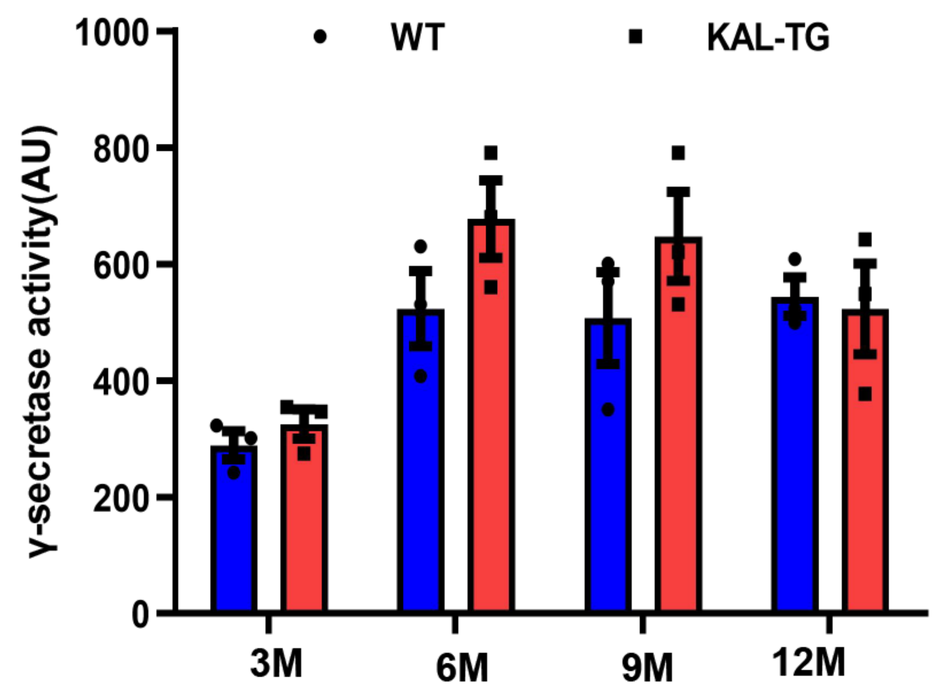

G

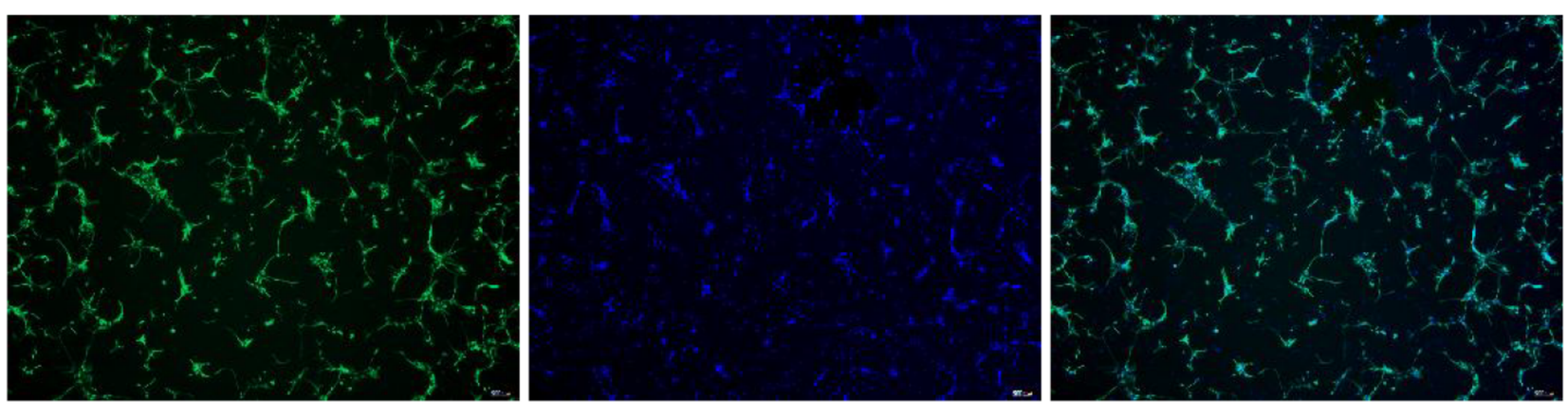

primary hippocampal neurons

Fig.S3

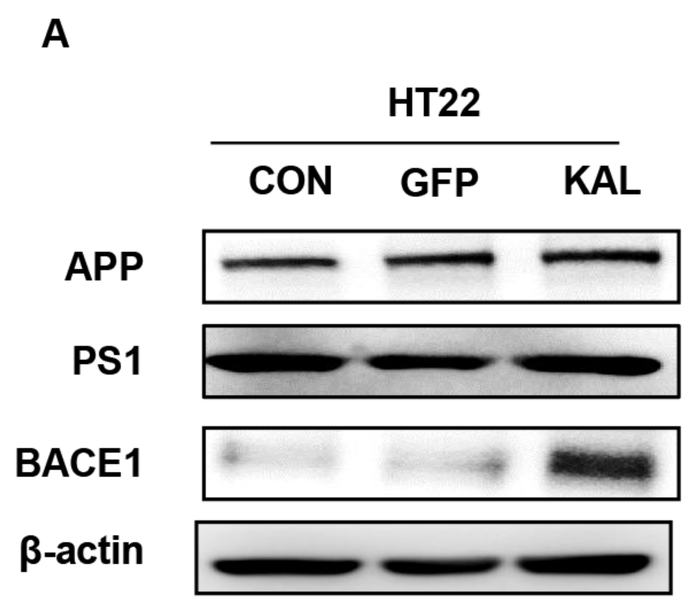
A
HT22
CON
GFP
KAL
APP
PS1
BACE1
β-actin

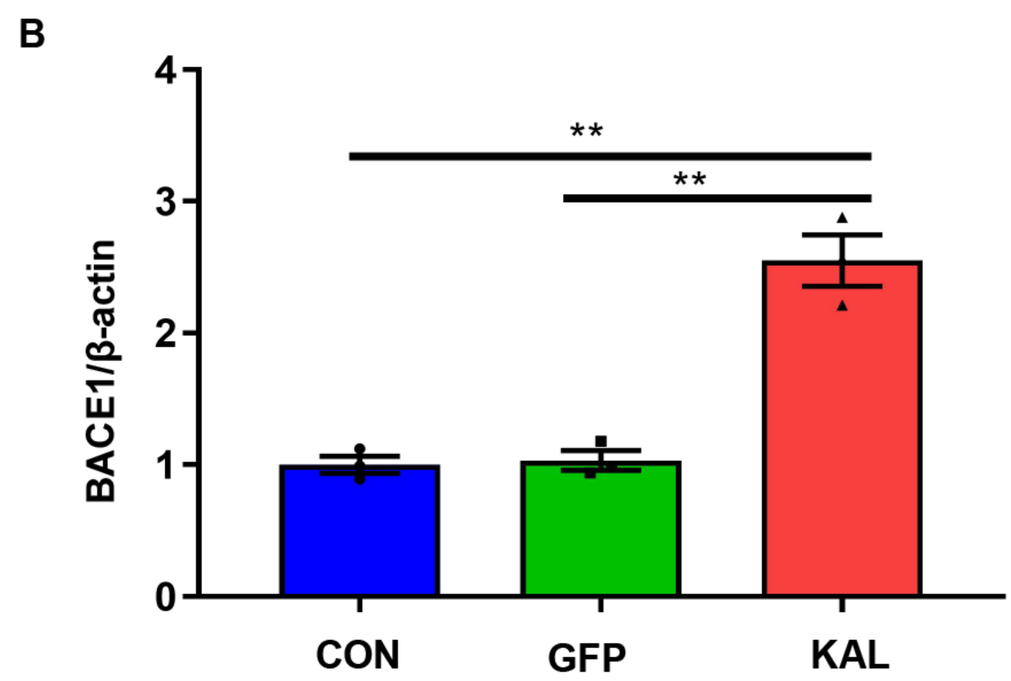
B
BACE1/β-actin
4
3
2
1
0
**
**
CON
GFP
KAL

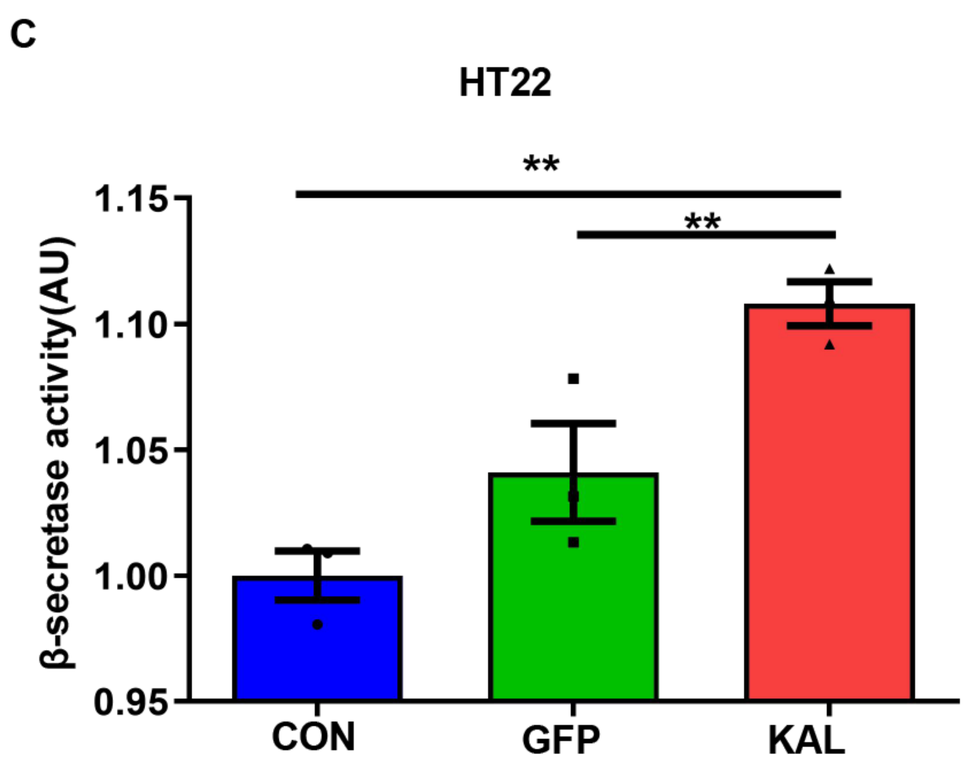
C
HT22
β-secretase activity(AU)
1.15
1.10
1.05
1.00
0.95
**
**
CON
GFP
KAL

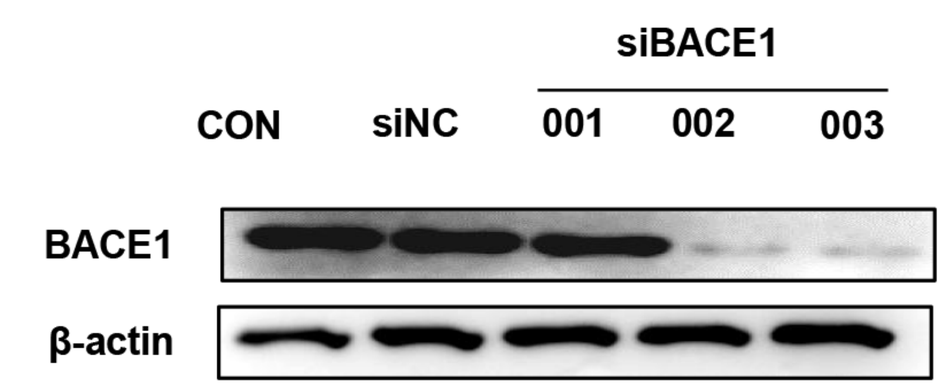
D
siBACE1
CON
siNC
001
002
003
BACE1
β-actin

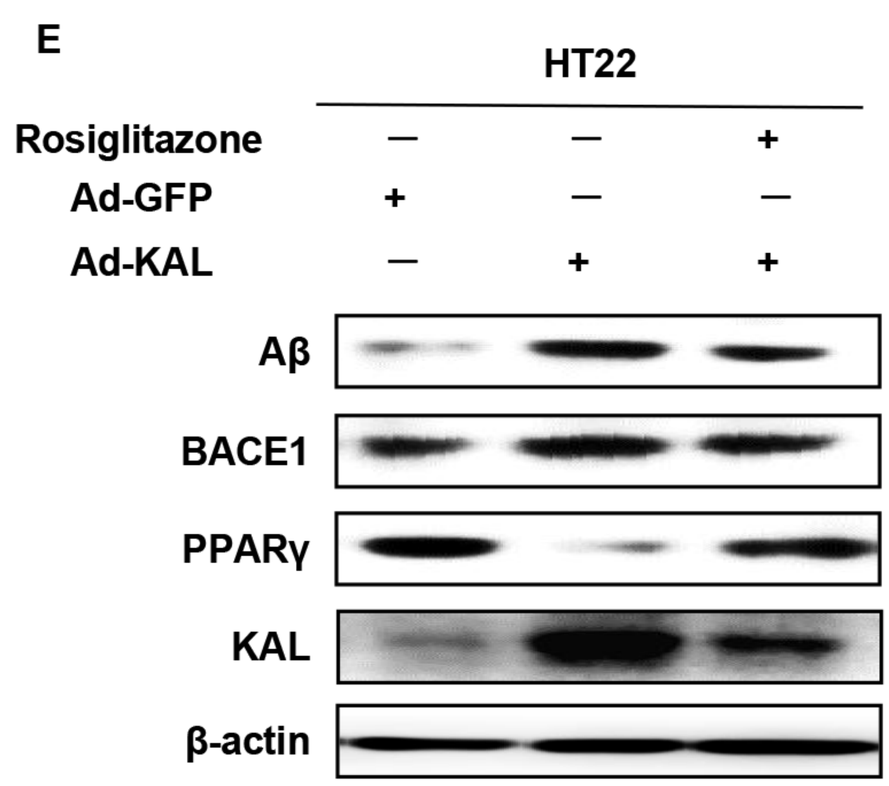
E
HT22
Rosiglitazone
Ad-GFP
Ad-KAL
Aβ
BACE1
PPARγ
KAL
β-actin

Fig.S4

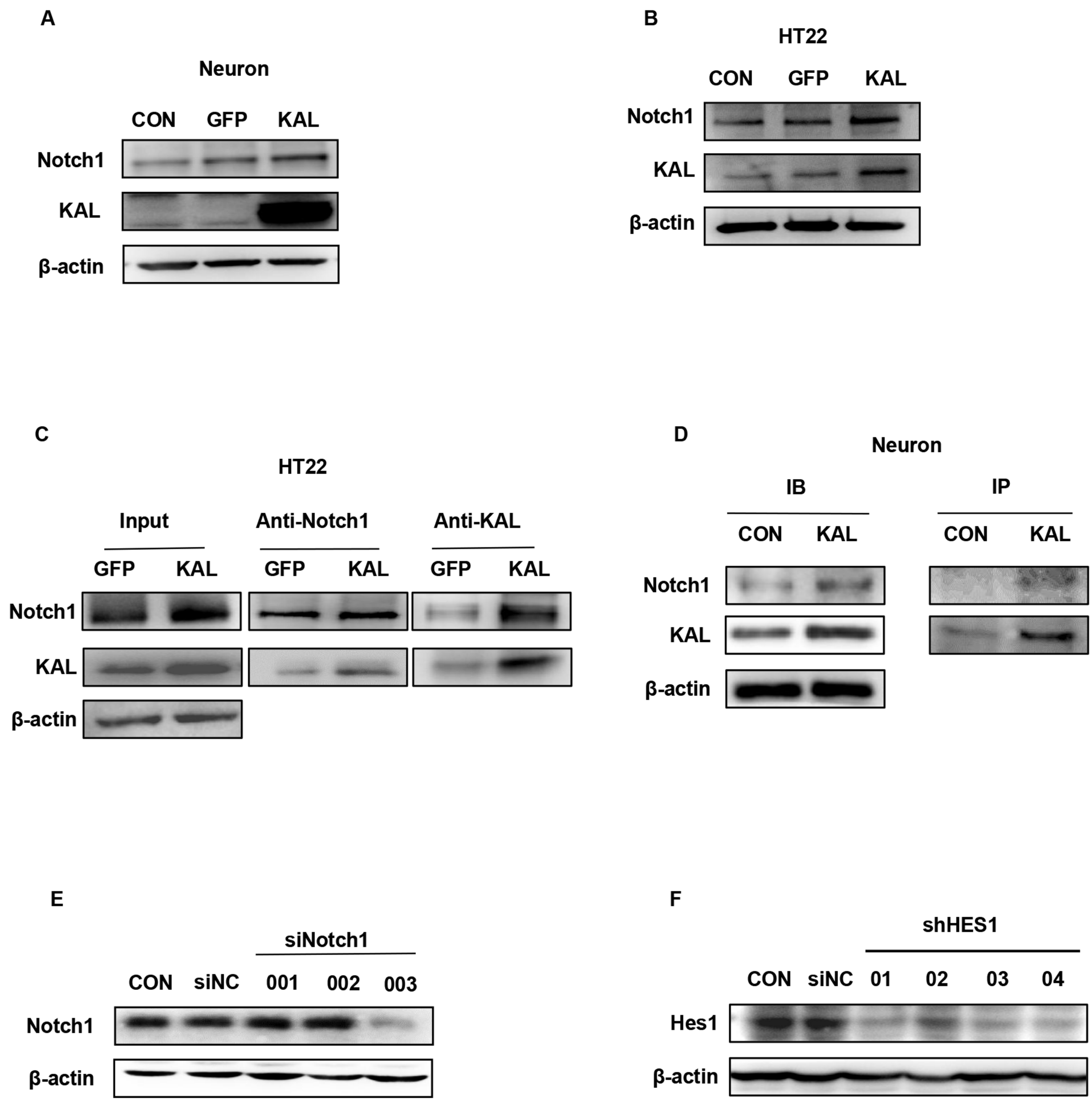
A
Neuron
CON
GFP
KAL
Notch1
KAL
β-actin
B
HT22
CON
GFP
KAL
Notch1
KAL
β-actin
C
HT22
Input
Anti-Notch1
Anti-KAL
GFP
KAL
GFP
KAL
GFP
KAL
Notch1
KAL
β-actin
D
Neuron
IB
IP
CON
KAL
CON
KAL
Notch1
KAL
β-actin
E
siNotch1
CON
siNC
001
002
003
Notch1
β-actin
F
shHES1
CON
siNC
01
02
03
04
Hes1
β-actin

Fig.S5

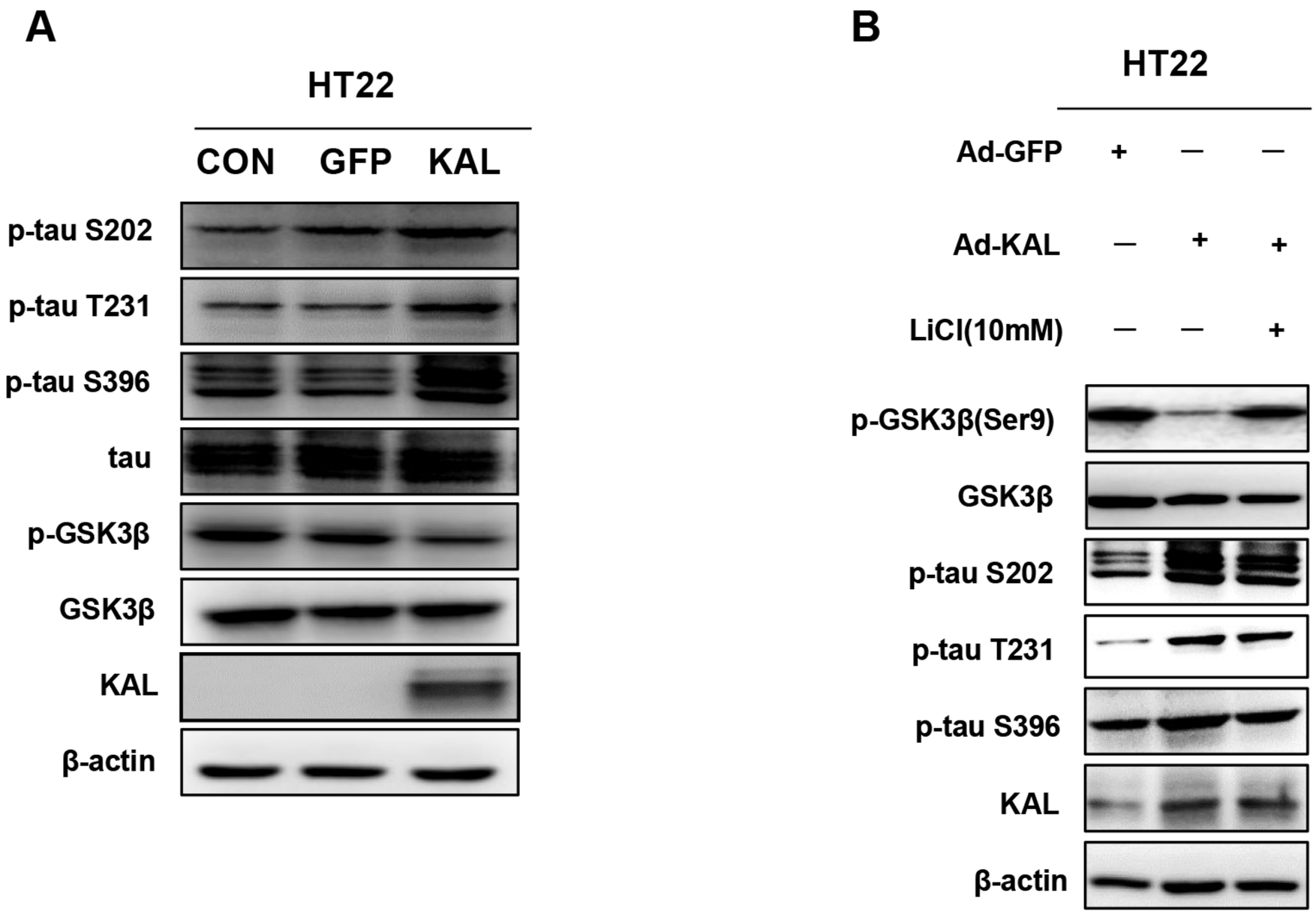
A
HT22
CON
GFP
KAL
p-tau S202
p-tau T231
p-tau S396
tau
p-GSK3β
GSK3β
KAL
β-actin
B
HT22
Ad-GFP + — —
Ad-KAL — + +
LiCl(10mM) — — +
p-GSK3β(Ser9)
GSK3β
p-tau S202
p-tau T231
p-tau S396
KAL
β-actin